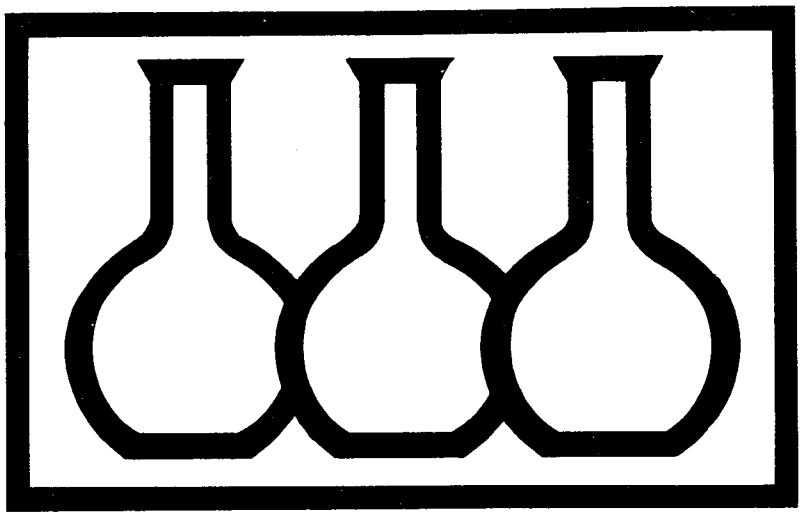

NIOSH RESEARCH REPORT

Ocular Ultraviolet Effects from 295nm to 400nm in the Rabbit Eye

U.S. DEPARTMENT OF HEALTH, EDUCATION, AND WELFARE
PUBLIC HEALTH SERVICE / CENTER FOR DISEASE CONTROL
NATIONAL INSTITUTE FOR OCCUPATIONAL SAFETY AND HEALTH

OCULAR ULTRAVIOLET EFFECTS

FROM 295 nm TO 400 nm

IN THE RABBIT EYE

University of Houston
College of Optometry
Houston, Texas 77004

Contract No. CDC-99-74-12

U.S. DEPARTMENT OF HEALTH, EDUCATION, AND WELFARE
Public Health Service
Center for Disease Control
National Institute for Occupational Safety and Health
Division of Biomedical and Behavioral Science
Cincinnati, Ohio 45226

October 1977

1a

Donald Graves Pitts, Ph.D.
Anthony Peter Cullen, M.Sc. (Ophth)
Principal Investigators

Pierrette Dayhaw Hacker, Ph.D.
Research Associate

Wordie H. Parr, Ph.D.
NIOSH Project Officer

DHEW (NIOSH) Publication No. 77-175

BIBLIOGRAPHIC DATA SHEET	1. Report No. NIOSH-77-175	2.	3. Recipient's Accession No.
4. Title and Subtitle OCULAR ULTRAVIOLET EFFECTS FROM 295 nm TO 400 nm IN THE RABBIT EYE			5. Report Date Oct. 1977
			6.
7. Author(s)			8. Performing Organization Rept. No.
9. Performing Organization Name and Address University of Houston College of Optometry Houston, Texas 77004			10. Project/Task/Work Unit No. 11. Contract/Grant No. CDC-99-74-12
12. Sponsoring Organization Name and Address National Institute for Occupational Safety and Health 4676 Columbia Parkway Cincinnati, Ohio 45226			13. Type of Report & Period Covered 14.

15. Supplementary Notes

16. Abstracts Pigmented rabbit eyes were irradiated with ultraviolet in 5 nanometer intervals from 290 to 320 nanometers and in 10 nanometer intervals from 325 to 400 nanometers. Occular tissues were studied with the electron microscope to localize and describe the morphology of the damage. The upper limit of the action spectrum for cornea was established at 320 nanometers. The most efficient waveband for lenticular damage was 300 nanometers which gave a radiant exposure threshold of 0.15 joules per square centimeter. The lenticular radiant exposure threshold produced transient lenticular opacities which disappeared within 24 hours to 2 weeks. Permanent cataracts occurred at radiant exposure levels approximately twice the threshold exposure. Radiant exposures of twice the threshold exposure for the cornea resulted in irreversible corneal damage in the form of stromal haze, stromal opacities, endothelial changes, and anterior uvitis. Preliminary studies on a primate at 300 nanometers gave a corneal threshold and a lens threshold of about 0.01 and 0.12 joules per square centimeter, respectively.

17. Key Words and Document Analysis. 17a. Descriptors
Electromagnetic radiation
Ultraviolet radiation
Electron microscopy
Eye diseases
Histology
Corneal opacity
Radiation injuries
Cataracts

17b. Identifiers/Open-Ended Terms 06/J

17c. COSATI Field/Group

18. Availability Statement	19. Security Class (This Report)	21. No. of Pages
Release unlimited	UNCLASSIFIED	90
	20. Security Class (This Page) UNCLASSIFIED	22. Price PCA05-A01

ABSTRACT

A 5000 x Xe-Hg source was used to produce 6.6 nm full-bandpass UV radiation through a double monochromator and 10.0 nm full-bandpass UV radiation through a single monochromator. Pigmented rabbit eyes were irradiated with UV in 5 nm intervals from 290 nm to 320 nm and in 10 nm intervals from 325 nm to 400 nm. Corneal and lenticular damage was evaluated and classified with a biomicroscope independently by two investigators. Ocular tissues were studied with the electron microscope to localize and describe the morphology of the damage.

The upper limit of the action spectrum for the cornea was established at 320 nm. The action spectrum for UV induced cataracts begins at 295 nm and extends to 320 nm. The most efficient waveband for lenticular damage was 300 nm which gave a radiant exposure threshold H_L of 0.15 Jcm^{-2}. The lenticular radiant exposure threshold produced lenticular opacities which were transient and disappeared within 24 hours to 2 weeks. Permanent cataracts occurred at radiant exposure levels approximately twice the threshold exposure ($2 \times H_L$). Radiant exposures of twice the threshold exposure for the cornea ($2 \times H_C$) resulted in irreversible corneal damage. Corneal damage included stromal haze, stromal opacities, endothelial changes, and anterior uveitis.

Preliminary studies on a primate (Galago senegalensis) at 300 nm gave a corneal threshold of 0.01 Jcm^{-2} and a lens threshold of about 0.12 Jcm^{-2}.

Areas in which further ultraviolet research should be accomplished are provided.

CONTENTS

ACKNOWLEDGMENTS

The authors wish to express their appreciation to Dr. Wordie H. Parr for his assistance in the direction and scope of the research accomplished under this contract. Dr. Parr has aided materially in the research protocol and data evaluation.

This manuscript is dedicated to the rabbits who have contributed to a research program designed to solve a human problem. While it has been said that rabbits feel it is good "to be petted a little, praised a little, and appreciated a little", the investigators are magnanimous in their praise and appreciation to these rabbits.

OCULAR ULTRAVIOLET EFFECTS

FROM

295 nm TO 400 nm

INTRODUCTION

Purpose of the Research

The purpose of the research was to establish the effects of ultraviolet (UV) radiation on the eye in the 295 nm to 400 nm wavelength range and to provide data from which protective criteria and effective standards may be established.

The following covers the morphology of the eye and the research on the effects and action spectra of ultraviolet radiation in the 300 nm to 400 nm wavelength range. The morphology of the eye is concise and is designed to acquaint the reader with the anatomical terminology to be used in the body of the report. The review of the literature served as the basis for the comparison and the discussion of ultraviolet radiation bio-effects as observed in this study.

Morphology and Histology of the Cornea and Lens

The gross morphology of the human eye is summarized in Figure 1. The gross anatomy of the eye in most animals does not differ greatly from the human eye except in specialized tissues. These differences will be emphasized in the text. Ultraviolet radiation under various conditions of exposure has been reported to affect the cornea, the aqueous, the iris, the crystalline lens, and the retina.

The anatomic features of the rabbit cornea will be given because most of the research on the ocular effects from exposure to ultraviolet radiation has been on the rabbit. The major difference between the rabbit and the primate and human corneas is the presence of Bowman's Layer. Bowman's Layer is prominent in the human and primate corneas but is only represented by a membrane-like structure in the rabbit cornea known as the basement membrane in the rabbit. Histologically, the rabbit cornea has five tissue layers. From externally to internally, the tissue layers are the epithelium, the basement membrane, the stroma, Descemet's membrane, and the endothelium (Figure 2).

The external layer of the epithelium is composed of five to six layers of stratified squamous epithelial cells. These cells and their oval, pale-staining, poorly outlined nuclei have their long axis parallel to the surface of the cornea and, in most histochemical preparations, have a much lighter appearance than the polyhedral and basal cells (Figures 3 and 4). Organelles remain distinguishable even in the outermost

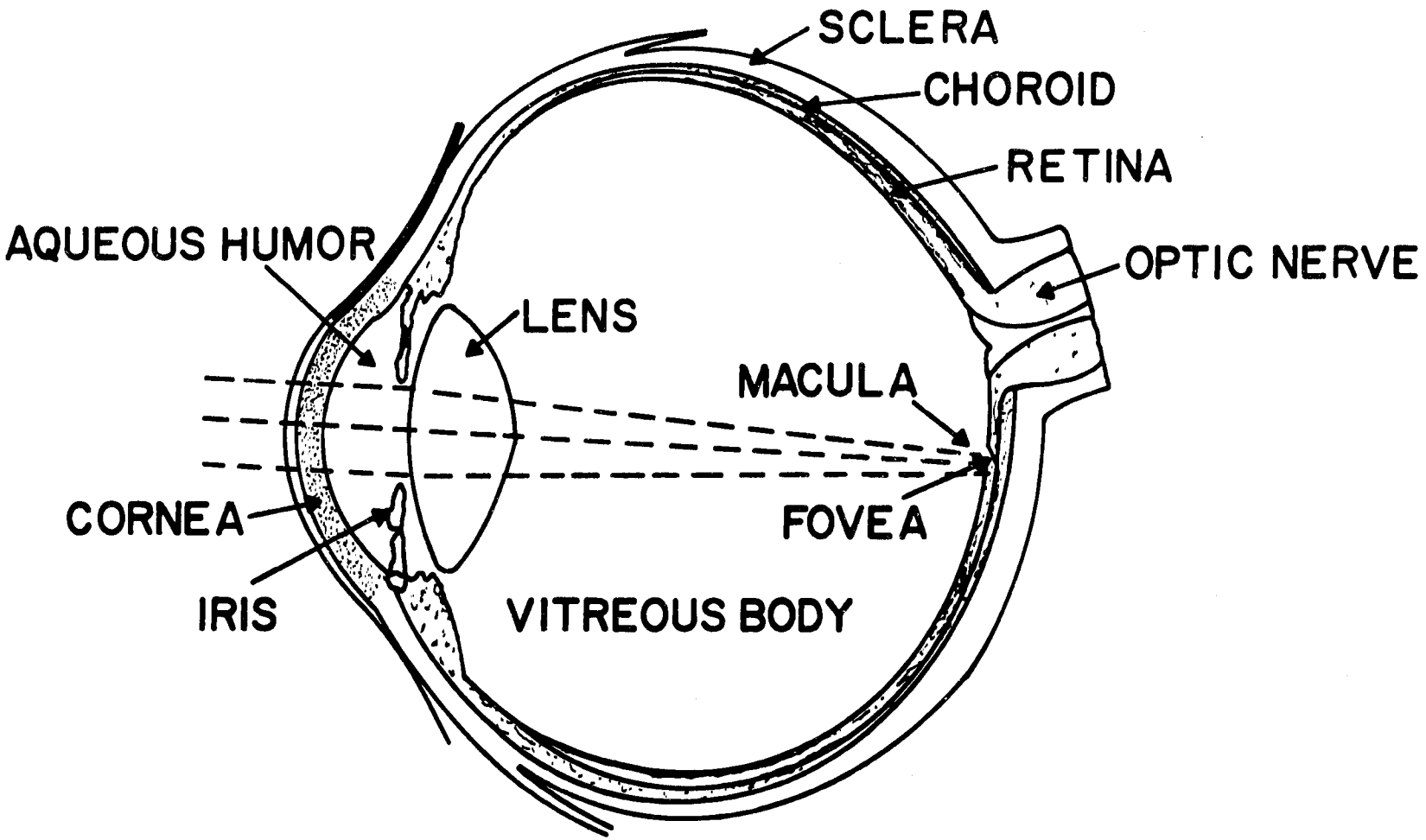

Figure 1: The gross structures of the human eye.

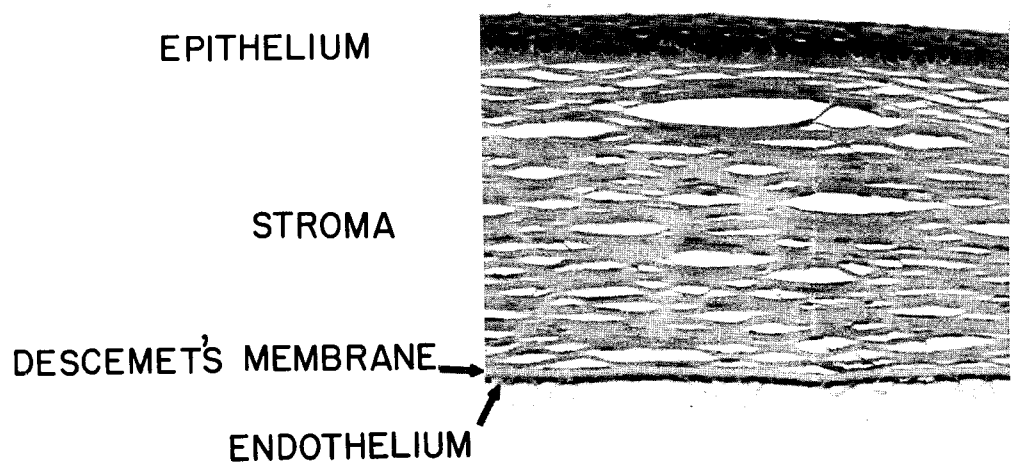

Figure 2: Histology of the normal rabbit cornea. Formalin-fixed, paraffin-embedded, 6 micrometers thick section (Gomori trichrome stain, 104 X).

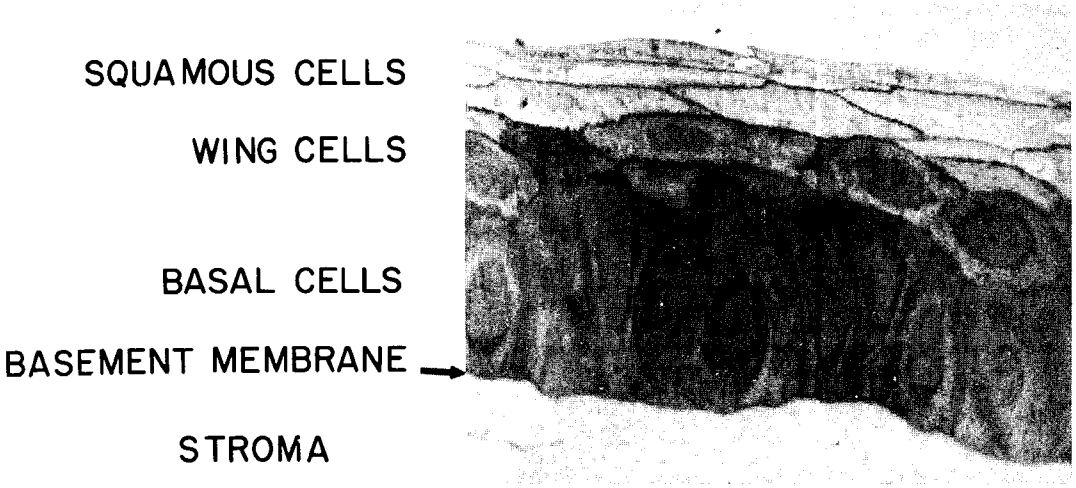

Figure 3: Corneal epithelium of a normal rabbit cornea as seen by oil immersion light microscopy in 1-micron-thick, Epon-embedded sections (Paragon stain, 1260 X).

squamous cells, where there is an increase in small vesicular structures in the perinuclear region. One or two cell layers of polyhedral shaped cells are seen just beneath the stratified squamous cells. These cells contain nuclei which are generally spherical and have irregularities in their profiles. The innermost layer of the epithelium is made up of basal cells which are columnar shaped and have oval nuclei generally located in the superficial portion of the cell. The basal, columnar cells contain large ellipsoidal to spherical nuclei oriented with the axis of the cell perpendicular to the corneal surface. Distinct, irregular, lobed nucleoli are frequently found in the nuclei of the epithelial cells and are composed of finely granular, moderately dense material.

Mitochondria, Golgi apparatus, and endoplasmic reticulum are seen in cells of all three layers of the epithelium but are most abundant in the basal layer where they are most often found in perinuclear areas (Figure 4). The randomly distributed ribosomes observed in all epithelial cells are most numerous in the basal cells. Membrane-bound dense bodies are also observed in the cytoplasm.

The cytoplasmic matrix of all three zones is composed of densely packed tonofibrils, some of which appear to attach to desmosomes. The tonofibrils are most prominent in the polyhedral and the superficial squamous cells. Numerous desmosomes are present along opposing membranes of adjacent cells of all layers. Adjacent to the basement membrane, dense, half-desmosome-like structures are located on the basal epithelial cells borders. The cell membranes of adajacent cells of all layers form projections which interdigitate with each other and give the cell borders a convoluted appearance.

There are no actual or artifactual intercellular spaces visible by light microscopy since all of the cells in the epithelium are closely knit. The normal epithelium contains no blood vessels or leukocytes. Occasionally, mitotic cells are found in the basal epithelial layers of the epithelium. The basal epithelial cells rest on a very thin basement membrane which is difficult to visualize by light microscopy. Bare nerve fibers are observed occasionally in the basal zone of the epithelium. Nerve fibers are not observed frequently in the superficial layers.

The human and the primate corneas demonstrate a much more prominent Bowman's layer.[1] The Bowman's layer of the human and primate corneas is composed mainly of collagen. The anterior surface of Bowman's layer blends with the basement membrane of the epithelium. Posteriorly, Bowman's layer becomes intertwined with the anterior lamellae of the stroma making the transition less distinct.

Abutting the basement membrane of the rabbit cornea is the stroma layer of substantia propria (Figures 2 to 4), which is avascular and is composed of collagen fibers. Interspaced between the collagen fibers are fibrocytes or keratocytes which have long filamentous nuclei and distinguishable cell borders. The stroma comprises approximately 85% of the corneal thickness. The stroma contains non-myelinated nerve fibers from which minute branches penetrate into the overlying epithelium in the rabbit cornea. The fine nerve fibers can be demonstrated only with special histologic techniques.

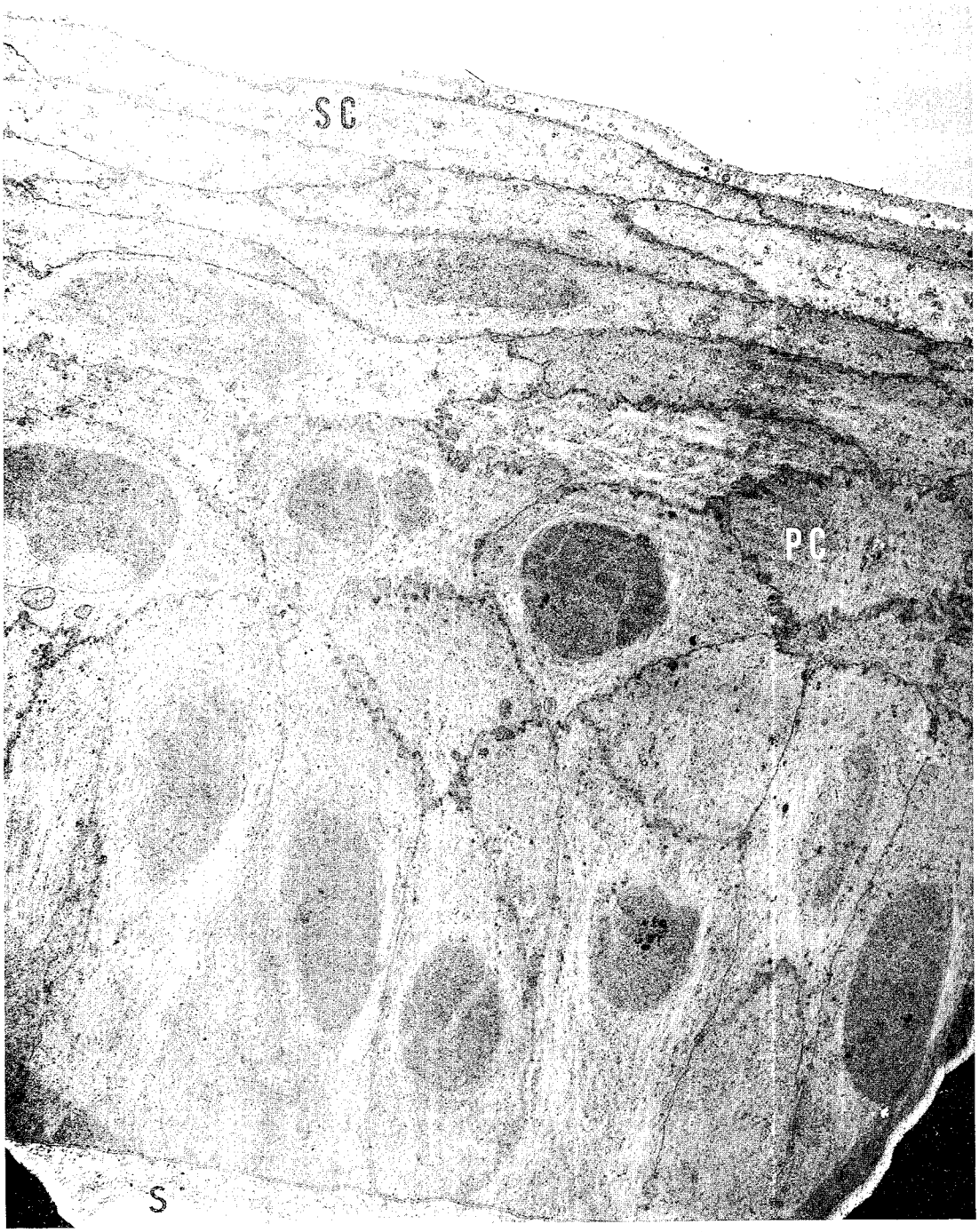

Figure 4a: Low-magnification electron micrograph of the normal rabbit corneal epithelium. Note the columnar-shaped basal cells (BC), the polyhedral cells (PC) in the mid-portion of the epithelium, and the outer squamous cells (SC). Cell organelles are not numerous, but cell borders are distinct. A portion of the stromal layer (S) is visible in the lower left corner (4040 X).

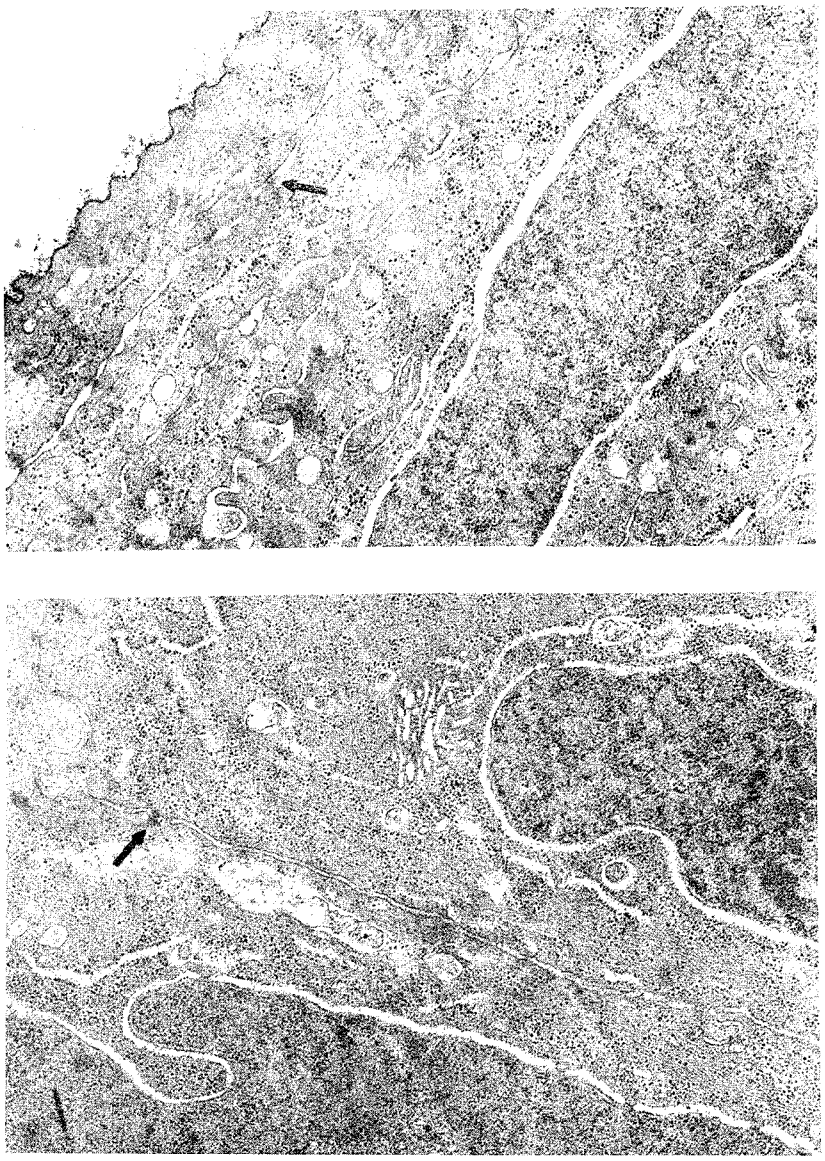

Figure 4b: Surface cells of normal rabbit epithelium. The surface layer of cells are flattened with numerous desmosomal attachments (arrow) between these outer cells. Microvilli protrude from the outermost surface. The cytoplasm contains the usual organelles, a rather large amount of glycogen and the membrane-bound vesicles characteristic of these cells (15,340 X).

Figure 4c: The nuclei of the wing cells have a flattened appearance than those of the basal cells. Note numerous desmosomes and interdigitations (15,340 X).

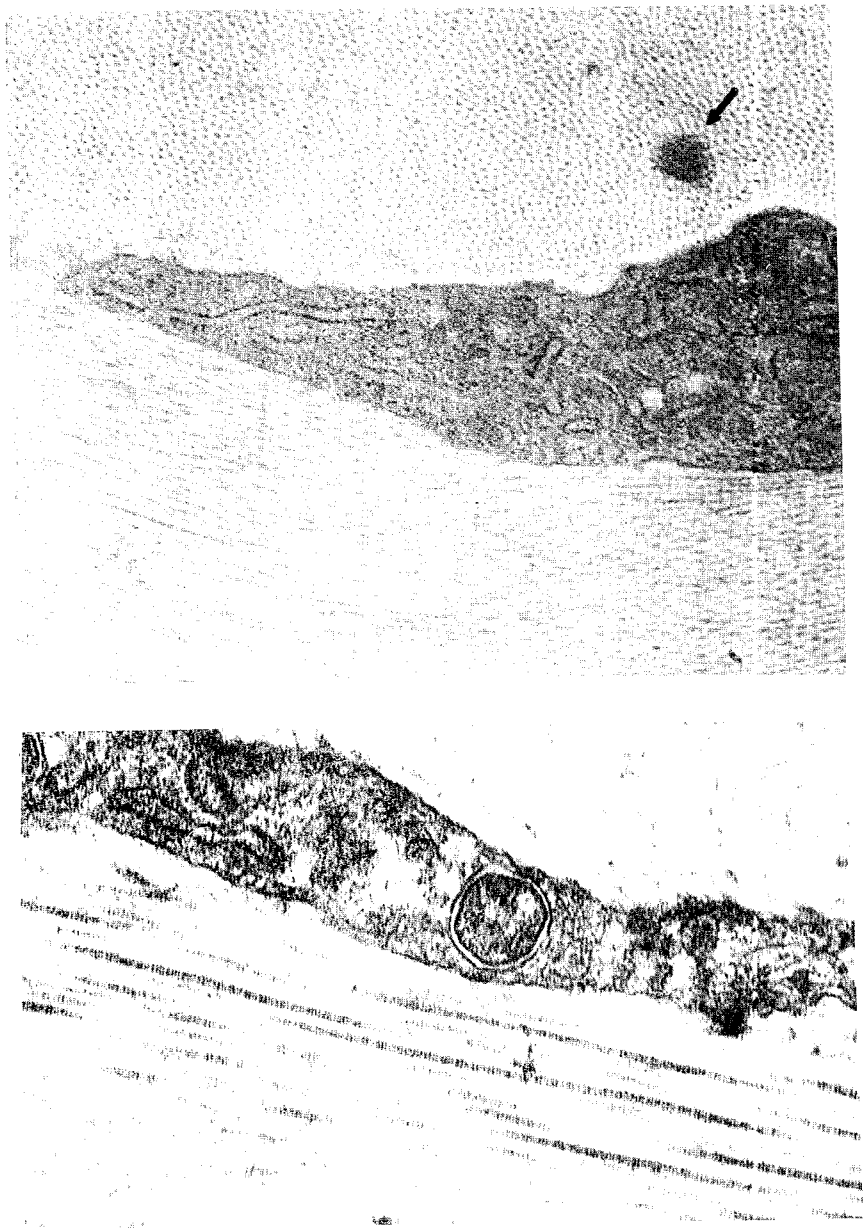

Figure 4d: The rabbit corneal stroma is composed of the typical collagen lamellae which run at right angles to one another. Note the regular arrangement of collagen fibers and the dense round mass (arrow) often found in collagenous tissue of the eye (33,000 X). The characteristic periodicity of collagen fibers is observed (52,000 X).

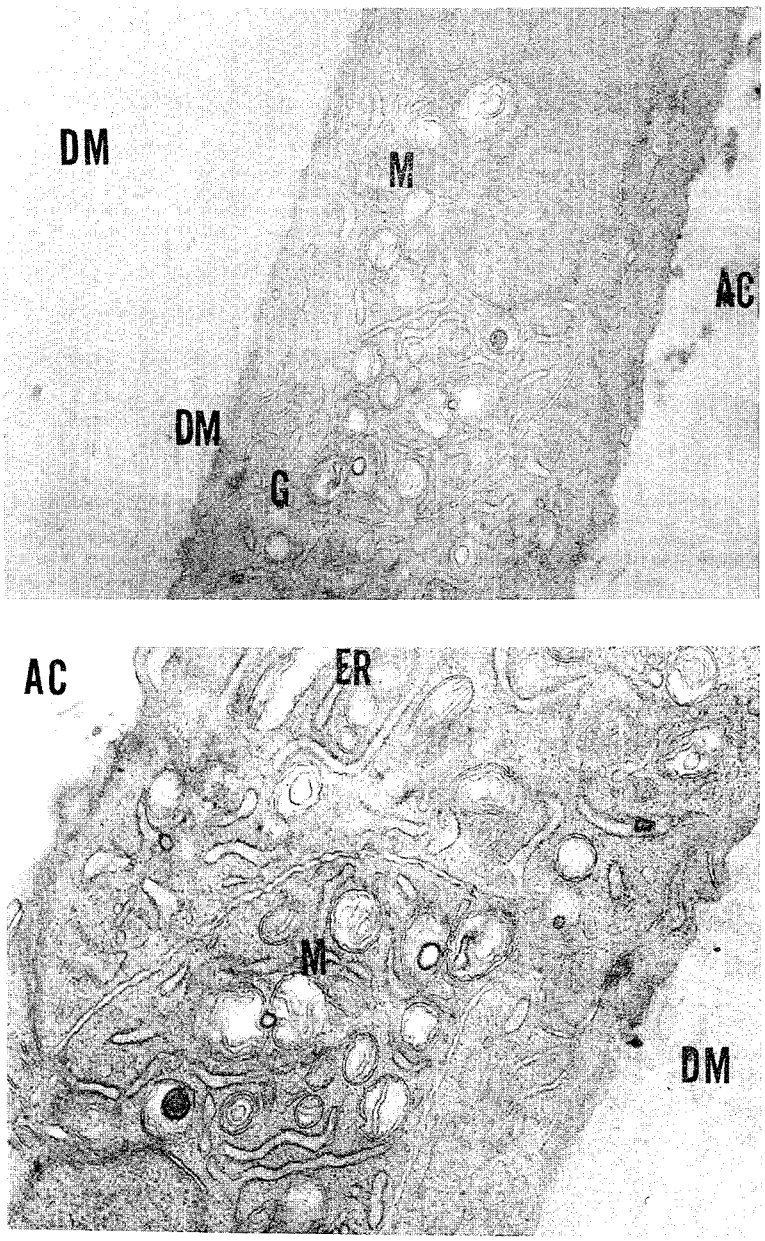

Figure 4e: The corneal endothelium of the rabbit is one-cell in thickness. A number of zona occludens are observed at the surfaces of neighboring interdigitating cells. Within the cells are numerous mitochondria (M) interspersed between rough endoplasmic reticulum (ER) and Golgi (G). Characteristic multivesicular bodies Descemet's Membrane (DM) and the Anterior Chamber (AC) can also be seen. (Upper 15,340 X; lower 23,600 X).

Descemet's membrane is positioned subadjacent to the stromal layer. Descemet's membrane is relatively uniform in thickness, 8 to 10 microns, and is composed of an amorphous PAS positive material. The final layer of the cornea is formed by a delicate single layer of cuboidal endothelial cells situated on the internal aspect of Descemet's membrane. The endothelial cells line the corneal surface of the anterior chamber of the eye.

The human crystalline lens has been selected for description since it's anatomy is well established and most mamallian lenses are similar to the human lens. The crystalline lens is a bi-convex structure situated just posterior to the iris and anterior to the vitreous body. The human crystalline lens is 9 to 10 mm. in diameter, 4 to 5 mm. thick and its anterior surface is less convex (9 mm. radius) than the posterior surface (5.5 mm. radius). There are some terms related to the lens which should be defined. The equator is the border where the anterior and posterior surfaces meet. The anterior pole lies at the center of the anterior surface and the posterior pole is located at the center of the posterior surface. The crystalline lens consists of the capsule, the anterior epithelium, the lens fibers, and the cement substance.

The capsule is a transparent, membranous envelope which encases the entire lens. It is highly elastic being thinner at the anterior and posterior poles, thicker at the equator and even thicker at the intermediate peripheral zones (Figure 5).

The anterior epithelium consists of a single layer of cuboidal cells which lie just underneath or posterior to the anterior capsule and cover the entire front surface of the lens (Figure 5). There is no posterior epithelium because the posterior epithelial cells filled the central cavity of the lens vesicle during the embryological development of the lens. The anterior epithelial cells gradually become columnar and elongate into fibers as they approach the equator. That portion of the anterior epithelial cell which is in contact with the capsule become the posterior portion of the fiber and the anterior part of the anterior epithelial cell becomes the anterior fiber. At the lens equator, the nuclei of the epithelial cells form an S-shaped zone of nuclei throughout the entire circumference of the lens.

The cement substance glues or holds the lens materials together and is not visible in ordinary histological sections. The cement substance lies beneath the capsule, deep to the anterior epithelium, and forms the central strand. The central strand runs somewhat like an axle from the posterior pole to the anterior pole of the lens. In addition, the axial cement substance projects three strands or rays toward the equator which divides the lens into at least three sectors. Under the biomicroscope, the strands of the cement substance form a "Y", with each arm being the same length, separated by 120 degrees and extending from the pole towards the equator. The anterior "Y" is vertical and the posterior "Y" is inverted (Figure 6A). The "Y's" are known as the anterior and posterior lens sutures. In the adult, the rays of the central strand may be much more complicated with as many as six primary and additional secondary lens sutures (Figure 6B). In spite of these complications, the fetal or original "Y's" persist throughout life in front of and behind the embryonic nucleus.

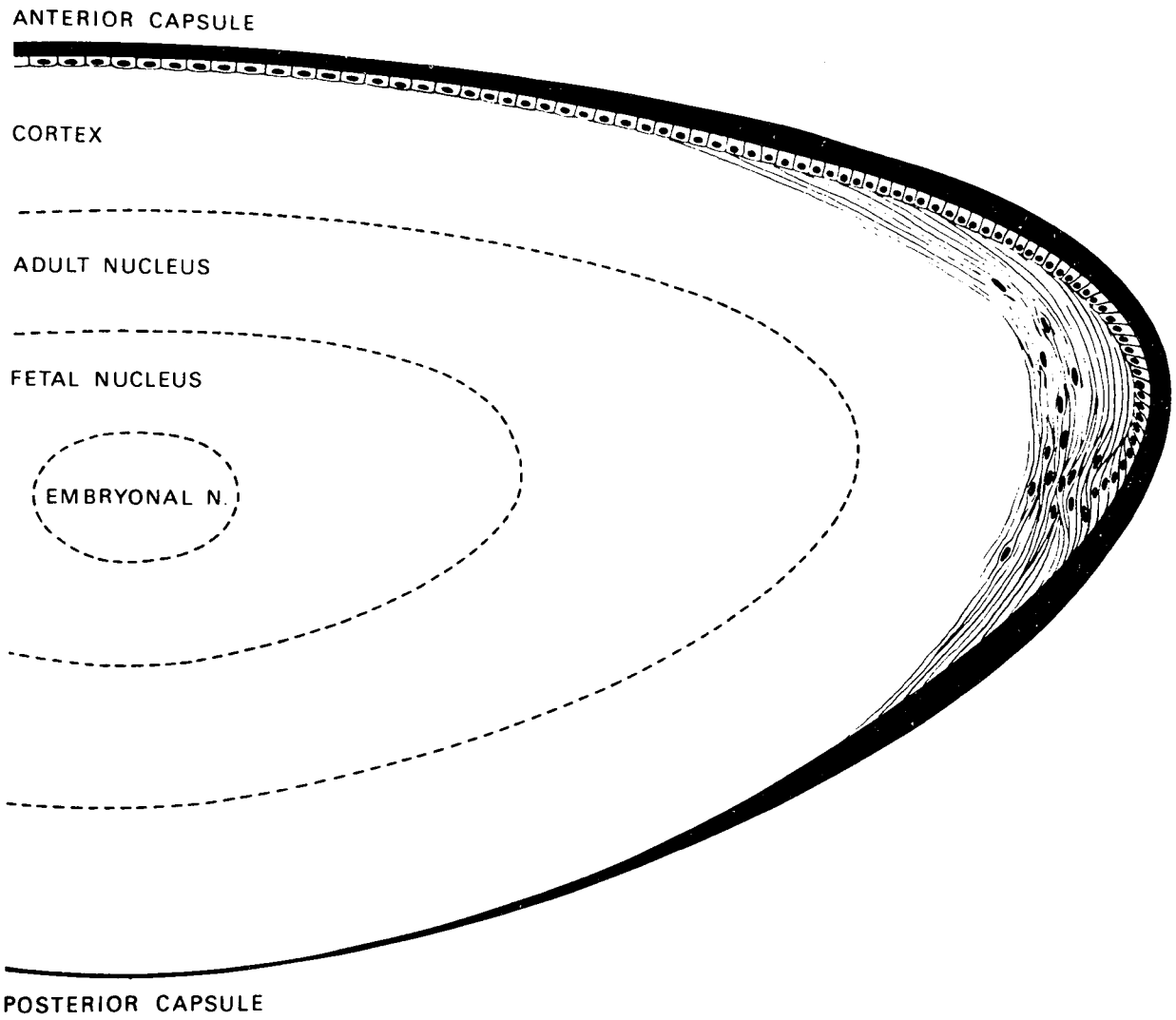

Figure 5: The capsule, anterior epithelium, cortex, and nuclear zones of the adult lens is schematically shown. Note the variations in the thickness of the capsule and the elongation of the anterior epithelium at the equator where lens fibers originate. (After Hogan, Alvarado, and Weddell[1]).

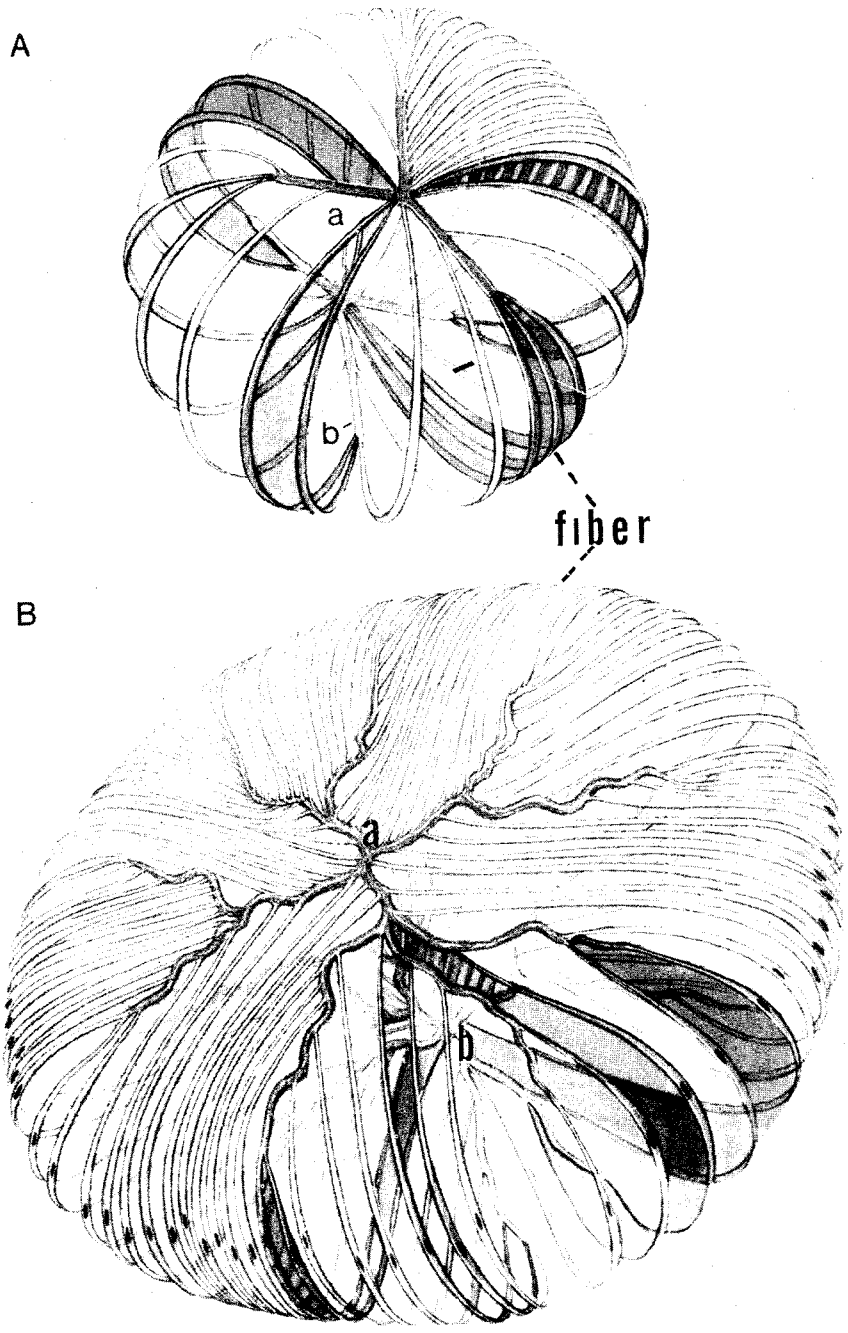

Figure 6: The embryonal and adult lens A shows the embryonal nucleus with the anterior Y at a and the posterior Y at b. The equatorial lens cells project their fibers to the tip of the Y suture at one surface of the lens and to the suture at the pose of the other surface of the lens. This relationship is maintained throughout the entire length of each suture.

B shows the adult lens cortex with a more complex suture organization. The fibers that arise from the tip of a branch of the suture insert farther anteriorly or posteriorly into the suture of the posterior pole. (After Hogan, Alvarado, and Weddell[1]).

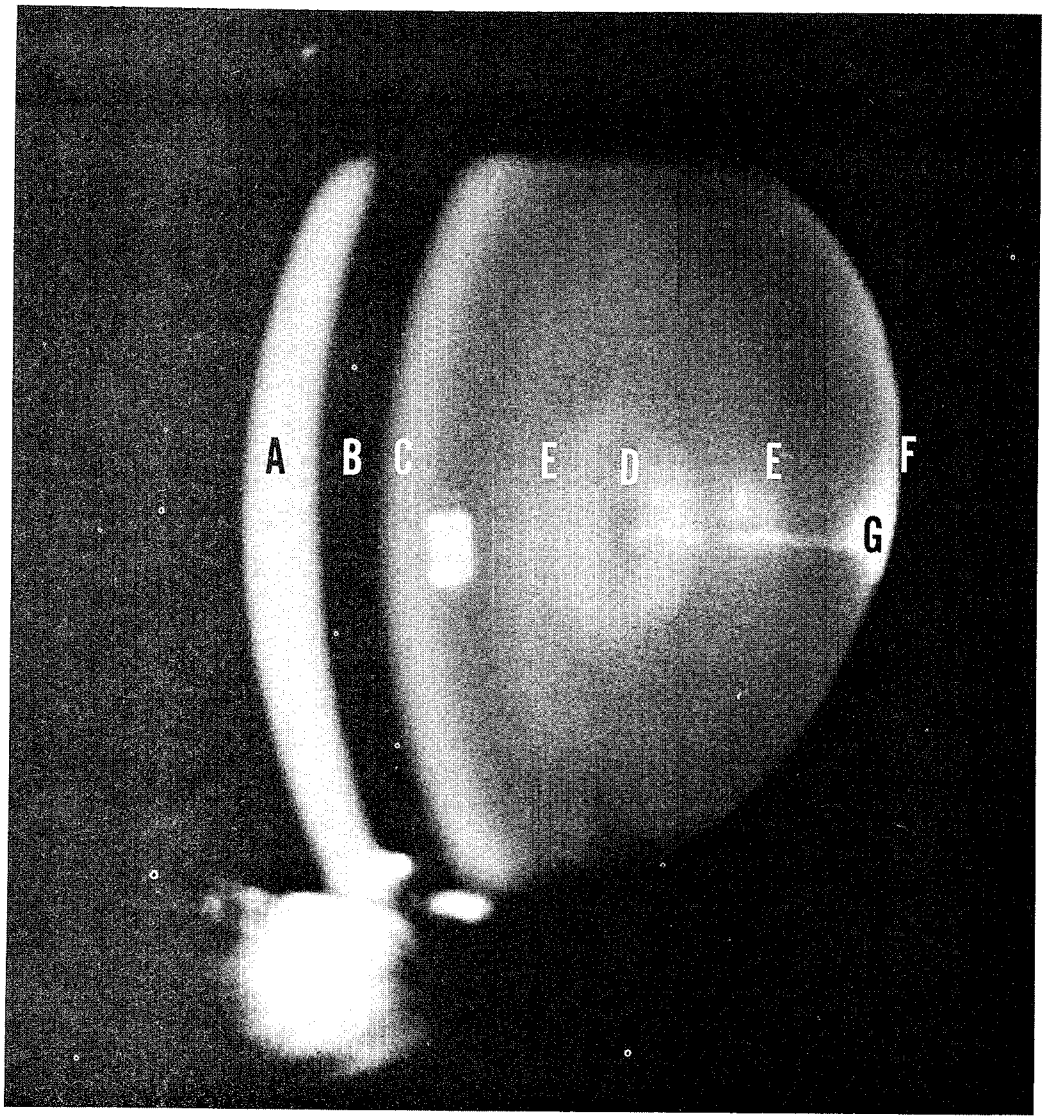

Figure 7: A biomicroscope photograph of the optical section of the cornea, the anterior chamber and the crystalline lens of the normal rabbit eye. The optical beam passes from left to right through the following components of the eye: A - Cornea; B - Anterior Chamber; C - Anterior Capsule and Anterior Epithelium of the Lens; D - Lens Nucleus; E - Lens Cortex; F - Posterior Lens Capsule; and G - Lenticular Opacity. See test for detailed description.

The lens fibers are long prismatic six-sided albuminoid material which taper as they reach the anterior or posterior sutures from the equator. The lens fibers are formed from the anterior epithelial cells located near the equator, radiate anteriorly and posteriorly, and their ends or tips insert into the rays of the strands of the cement substance. Newer fibers are formed externally to the old fibers and force the old fibers toward the center of the lens in concentric layers as a part of the aging process. The older fibers lose their nuclei as they are pushed centrally.

The unique growth process of the lens fibers causes the lens to take on the appearance of two zones. The external zone consisting of the relatively new nucleated fibers is called the cortex. The internal zone consisting of the old non-nucleated denser fibers is called the nucleus (Figure 5). As previously discussed, any injury, osmotic imbalance, alteration in lens metabolism, or alteration in lens proteins results in cataracts.

There is a major difference between the crystalline lens of the rabbit and of the human. The anterior suture of the rabbit lens is a single almost vertical whitish strand, canted slightly caudally superiorly, and cranially inferiorly. The posterior suture of the rabbit lens is a single whitish horizontal strand. Both sutures of the rabbit lens extend almost the entire length of the lens diameter.

Figure 7 shows a biomicroscopic photograph of the anterior segment of the normal rabbit eye. The optical beam passes from right to left through the cornea, anterior chamber and the crystalline lens. The different components of the lens are readily seen. Of particular interest is the posterior subcapsular opacity seen at G which projects a filament anteriorly to the nuclear opacity seen at D. The cortex E is clear except for the filament at G. The rectangular white spot just posterior to the anterior capsule and anterior epithelium is an artifact from the photographic flash.

For a more detailed and elegant description of the anatomy and histology of the eye, the reader is referred to Hogan, Alvarado, and Weddel[1].

The ultraviolet wavelengths above 290 nm are largely transmitted by the cornea leaving the underlying lens and iris exposed to UV. The lens absorbs essentially all of the UV radiation in the wavelength range from 295 nm to 365 nm and it is the ocular tissue especially susceptible to UV exposure (Figure 8). Therefore, the possible induction of lenticular cataracts in humans by exposure to ultraviolet radiation above 290 nm is of major concern. Any alteration of the crystalline lens or its capsule which results in decreased light transmittance or increased scattering of the visible spectrum may be called a cataract. Minimum alterations may not result in a change in vision although changes may be detected by a careful biomicroscopic examination. The term cataract is often clinically reserved for a symptomatic decrease in vision. Marked alterations of the lens and capsule invariably results in reduced or severely impaired vision. Cataracts may result from:[4,5]

1. Injury to the anterior lens epithelium which differentiate into lens fibers. These fibers become abnormal and reduce transmittance or increase the scatter of

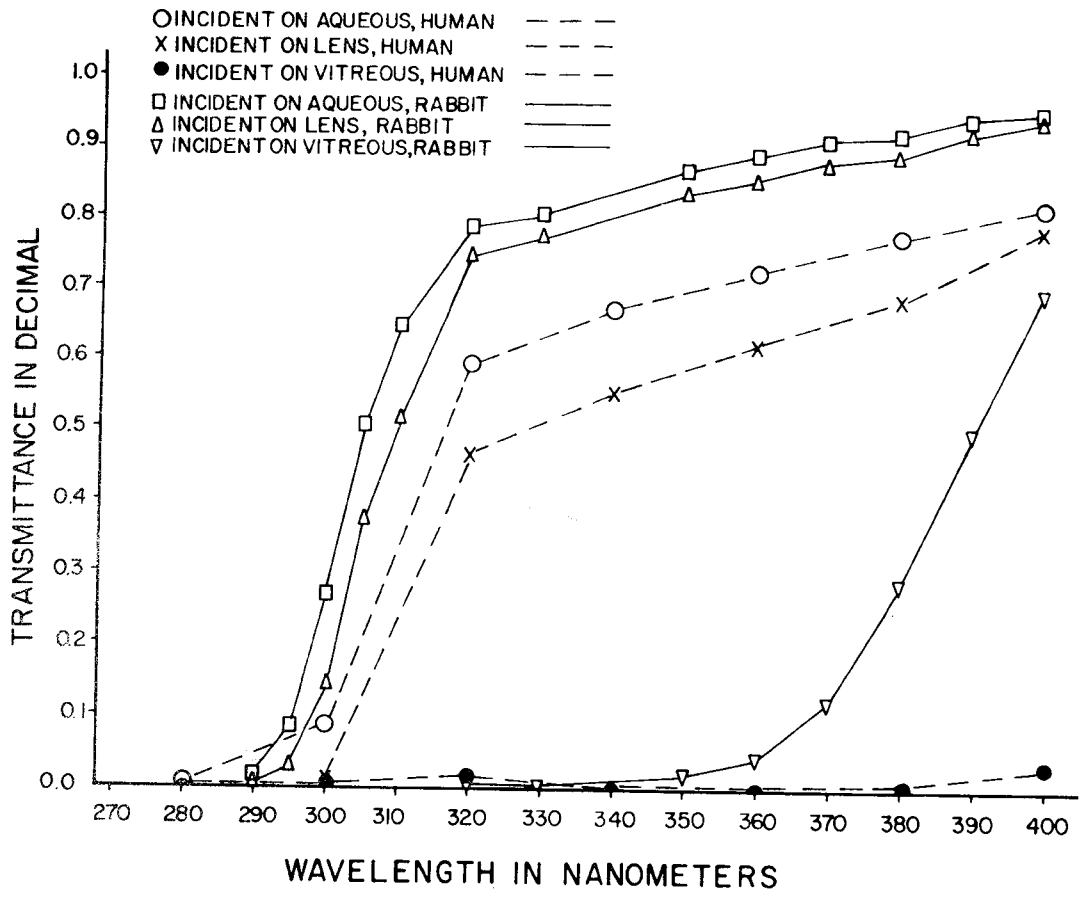

Figure 8: Comparison of rabbit and human transmittance of ultraviolet through the cornea, aqueous humor, crystalline lens, and incident of the vitreous. Most of the wavelengths below 300 nm are absorbed by the cornea while the wavelengths between 310 and 390 are absorbed by the lens (after Boettner and Wolter,[2] Kinsey,[3] and Bachem[15].)

incident visible light. Injury alterations usually are not evident immediately because the lens fibers differentiate slowly. Corticosteroid induced cataracts are felt to be the result of changes in the lens fiber synthesis.

2. Acute osmotic imbalance which results in water being drawn into the lens and an increased scatter of visible light occurs. Examples are traumatic, chemical, and thermal injury to the lens.

3. Alteration of the lens metabolism which results in changes in water, calcium, sodium, potassium and phosphate content as well as a decreased transmittance of visible light.

4. Alteration of the lens proteins resulting in localized changes in the refractive index of the lens material and increased light scatter. The senile cataract is thought to be such a mechanism.

There is relatively little knowledge about the basic mechanisms or fundamental changes which result in the cataractogenic process.

Review of the Literature

There is little quantified research data available which may be used to establish the ocular effects of exposure to the near UV spectrum between 300 nm and 400 nm. [6, 7] A review of the pertinent literature is presented to demonstrate the need for research in this area of the UV spectrum.

Verhoeff et al [8] used a quartz mercury lamp operating at 3.5 A and 90 V across the terminals of the tube. The lamp produced 65% of the total radiant flux in the UV range. At 59 cm from the lamp, the total abiotic irradiance was 4.2×10^{-4} Wcm^{2} of which 2.1×10^{-4} Wcm^{-2} was above 295 nm. It was stated that 3 minutes provided a liminal exposure. Verhoeff's threshold exposure for wavelengths greater than 295 nm was 3.78×10^{-2} Jcm^{-2} radiant exposure for the rabbit cornea. It is interesting to note that with exposures below 5 minutes (6.3×10^{-2} Jcm^{-2}) Verhoeff does not describe lenticular changes for these exposures. All exposures of 5 minutes or greater are described as showing abiotic changes in the lens eipthelium in as little as 24 to 48 hours. The lenses showed marked changes in the epithelium and the lens substance was affected, but only at a depth of about 20 µm beneath the capsule. Lens epithelial changes reached their maximum in 48 to 72 hours and included swelling of cells, appearance of granules in the cytoplasm, and the formation of a peripheral wall of cells. The peripheral wall consisted of a ring of deeply staining cells at the periphery of the exposed area. The nuclei of the lens epithelium cells remained normal, in spite of the above signs, except with intense exposures.

At 10 to 12 days after exposure, the lens epithelial cells lost their swollen appearance and the granules almost entirely disappeared. The nuclei were of various sizes and

shapes rather than the usually observed constant size. These capsular changes persisted up to 2 months after exposure. It is interesting that Verhoeff does not give information on changes in the lens substance which would result in lenticular opacities.

An important but often ignored finding of Verhoeff's study was that the corneal endothelium was destroyed when exposed to wavelengths longer than 295 nm for 6 to 12 minutes. The corresponding radiant exposure would be 7.56×10^{-2} Jcm^{-2} and 15.2×10^{-2} Jcm^{-2} respectively. Loss of the endothelium resulted in a marked swelling of the corneal stroma reported to be as much as 200%. The endothelium may be the key to threshold damage to ultraviolet above 295 nm.

Trümpy[9] exposed rabbit eyes to UV wavelengths from 280 to 435 nm but did not provide calibration data for the source. He observed qualitative lenticular changes which could not be compared to previous data. Van der Hoeve[10] criticized the research of Trümpy and compared Trümpy's work with previous data. The cited references by van der Hoeve will not assist materially in quantifying the radiant exposure threshold of UV in the 300 nm to 400 nm waveband range.

Duke-Elder[11, 12] provided a summary of research on the ocular effects of UV radiation up to 1929. In addition, Duke-Elder exposed rabbit corneas to a quartz mercury lamp operated at 204 volts and 0.67 amperes for a period of 10 minutes at a distance of one foot from the source. The unexposed eye was used as the control. The animal was sacrificed and the eyes studied histologically at various periods of time from two hours to ten days after exposure. At four hours, the effects consisted mainly of an occasional swelling of the external squamous and basal epithelial cells. The endothelium and stroma were normal. After six hours, the eosin stain showed that a large number of nuclei were red and the basal cells were widely spaced indicating edema. The superficial cells became irregular. The changes progressed and became most noticeable at 12 hours. The nuclei of the epithelial cells took on red stain and granules appeared to fill the entire nucleus which was usually surrounded by a vacuole-like space. In contrast, other cells remained normal. Desquamation proceeded in the central corneal area. The nuclei of the corneal stroma stained deeply with methylene blue and began to fragment. The effects increased in severity through 16 hours after exposure when swelling of the lamellae of the stroma was apparent.

At the 24 hour stage, the stroma showed a few granules, the lamellae were swollen and the endothelium showed some staining similar to the remainder of the cornea but did not exfoliate. There were few changes from the 24-hour state through 36 hours after exposure. The epithelial cells began to take on an orderly arrangement and the changes progressed slowly until in 7 days the cornea was essentially normal.

In addition to corneal changes, Duke-Elder reported changes in the aqueous humor, iris, lens and retina. The aqueous humor showed a marked increase in proteins, a slight increase in sugar but a decrease in the chlorides. The iris appeared congested after 12 to 16 hours and showed a disturbance of the iritic pigment. All iris conditions returned to normal within 80 hours. The lens showed the typical intercellular changes in the

pupillary area of the anterior epithelium just beneath the capsule about 13 to 36 hours after exposure. The anterior lenticular epithelium returned to normal within 10 days after exposure. The lens, stroma, and nucleus demonstrated fibers which were swollen and had lost their orderly arrangement.

The lens changes were attributed to be "purely chemical" in nature from the ultraviolet wavelengths of the spectrum. Although the initial anterior subcapsular lenticular changes were reversible, the final result should be an impairment of the semi-permeability of the capsule which would disturb the metabolic process of the system and result in long range permanent damage. Retinal damage was restricted to the region of the posterior pole of the eye. The retinal picture consisted of a disintegration and chromatin bleaching of the ganglion cells, a swelling of the nuclei of the inner nuclear layer, slight if any changes in the outer nuclear layer, and a normal rod and cone layer. The most marked changes were found from 8 hours to 20 hours after exposure. The retina returned to normal within 50 hours to 60 hours after exposure.

The ocular reactions reported by Duke-Elder may be considered rather severe but appear to be reversible. The total irradiance, spectral irradiance, and wavelength range of the source were not given. Therefore, it would be difficult to compare these radiant exposures with the data of other researchers investigating ocular damage from ultraviolet exposure. The report does provide important information on the destructive and reparative processes which can result from exposure of the eye to ultraviolet radiation.

Buschke et al's[13] research emphasized the destructive effects of ultraviolet on the nucleus of corneal epithelial cells, the loss of adhesion of the epithelial cell to Bowman's membrane, and the inhibitory effects of ultraviolet radiation on the healing process of the cell after exposure by observing changes in the mitotic activity of the epithelial cells.

Fischer et al[14] used narrow bandwidth UV from 250 nm to 350 nm and observed a change in the reflex-image of the cornea. They established 4.5×10^{-1} Jcm^{-2} as the threshold at 350 nm for the rabbit eye. The source was either a carbon arc or a tungsten strip-lamp passed through a double monochromator. A thermopile was used for calibration purposes. The irradiance varied from 0.2 to 2.0 Wcm^{-2} and the duration of exposures varied from 20 to 60 minutes. Fischer et al do not provide a sufficient description of their observations to determine if the exposures above 300 nm can actually be compared with other data. They did not use a biomicroscope to observe lenticular and aqueous changes.

Bachem,[15] using a filtered UV spectrum, concluded that exposure to repeated high dosages of longer UV wavelengths can cause cataracts through cumulative effects. He reported that the action spectrum for cataracts begins abruptly between 293 nm and 297 nm, reaches a peak near 297 nm, and falls abruptly near 313 nm. Minimal effects exist through a remainder of the near UV. In both the rabbit and guinea pig, reversible lenticular "blurring" occurred 5 to 10 days after exposure. With repeated "excessive" exposures to a waveband extending from 297 nm to 365 nm, irreversible lenticular

opacities occurred after a latency period which varied between 2.5 to 15 months. Bachem presents in tabular form the threshold values for lenticular opacity in the rabbit. While a bandwidth with 254 nm predominating was unable to produce a lenticular opacity, a waveband containing 297 nm and 289 nm required 2.0×10^{-1} Jcm^{-2} total exposure to produce a lenticular opacity. A waveband containing ultraviolet only above 302 nm required a 1.5×10^{1} Jcm^{-2} total exposure for a lenticular opacity. Finally, the spectral range from 334 nm to 365 nm required 5.0×10^{3} Jcm^{-2} radiant exposure to produce an opacity. Bachem concluded that daylight contained none of the far ultraviolet and far infared and, since both the visible and near infrared are freely transmitted by the ocular media, it would appear that the near ultraviolet was responsible for cataracts.

Bachem's threshold dosage in Jcm^{-2} was as follows:

Reaction	Containing 297-289+nm	Only above 302 nm	334-365 nm only
Rabbit lens, opacity	2.0×10^{-1}	1.5×10^{1}	5.0×10^{3}
Guinea-pig lens, opacity	1.0×10^{-1}	1.0×10^{1}	5.0×10^{3}
Guinea-pig, lens cataracts	3.0×10^{-1}	*4.0×10^{1}	3.0×10^{4}

*Cumulative from repeated applications

It is evident from the variability of the above-cited research that a threshold value for the 300 nm to 400 nm spectral range has not been established. Verhoeff et al arrived at 6.3×10^{-2} Jcm^{-2} radiant exposure for wavelengths above 295 nm while Fischer et al found a 4.5×10^{-1} Jcm^{-2} threshold at 350 nm. Both research groups used different criteria and it appears that Verhoeff et al actually produced lenticular and endothelial damage while Fischer's group demonstrated only corneal damage. In contrast, Bachem found a lenticular threshold of 1.5×10^{1} Jcm^{-2} for the waveband above 302 nm and 5.0×10^{-1} Jcm^{-2} for the 334-365 nm waveband range. Bachem's observations are based on a minimal number of positive findings and, therefore, his threshold values may not be comparable to other data.

The photochemical and biochemical mechanisms underlying the response of the eye to ultraviolet radiation above 300 nm have revealed some significant alterations in the proteins of the lens. Biochemical alterations of the lens also occurs with aging and cataract formation.

Clark et al[16] and Lerman[17] reported that the level of the insoluble protein albuminoid in the normal human crystalline lens increases from a minimum of about 3% below the age of 10 to about 40% at the age of 80 to 89. This level of insoluble protein increases to about 70% for the human lens nucleus with advanced brunescent and nigrescent nuclear cataracts. There was also a large decrease in the concentration of the smaller γ-crystalline protein, a small decrease in β-crystalline protein and an increase in the large α-crystalline protein. Thus, the changes in crystalline proteins with age have been fairly well established. It is possible that an increase in insoluble proteins produced by long UV exposure may increase light scattering within the lens.

Lerman's research indicated that the activation spectrum of γ-crystalline was well within the UV absorption spectra of purified fluorogen. Fluorogen shows a maximum absorption at 277 nm, a small absorption at 305 nm, and a fairly significant absorption peak at 370 nm. It is well known that lens fluorescence increases as the human becomes older. Lerman hypothesizes that the fluorescent material could be derived from tyrosine or tryptophan which are residues in the γ-crystalline molecule. Further, the fluorogen could be formed by a photooxidation process from UV light between 340 nm and 380 nm. This spectral band of UV is readily transmitted by the cornea and aqueous and readily absorbed by the crystalline lens (Figure 8). Lerman further states that the S-S linkages and the C-S linkages are involved in the formation of the albuminoid fraction. He postulates that fluorogen polymerization and decreased solubility add to some of the urea-insoluble albuminoid fraction.

Specific amino acids of lens protein and their photooxidation products may be involved in the cataractogenic process or lens protein may become linked to metabolically derived chromophores which absorb the long ultraviolet and act as photosensitizers. Free aromatic amino acids may be photooxidized into pigmented compounds with strong binding affinities for lens protein. Yellow-brown coloration of lens material may result and this material may play a role in the formation of brunescent cataracts.[18] Long ultraviolet absorbing pigment and fluorescent substances have been found to be covalently linked to specific peptides of lens protein.[19] As noted in humans, lens fluorescence increases with age.

A number of studies have suggested that tryptophan plays a pivotal role in UV induced changes in the lens. N-formylkynurenine, a photooxidation product of tryptophan[20, 21] is present in human lens[22] and can photosensitize further tryptophan oxidation by UV.[20,21] Tryptophan is photolyzed by UV into many unidentified pigmented and fluorescent compounds[23, 24] some of which bind to human and animal lens protein in vitro altering the physical and chemical properties of these proteins.[25]

Pirie[26] and van Heyningen[27] feel that the whole-lens protein are photooxidized by virtue of destruction of tryptophan groups in the protein. Pirie suggested that photooxidation probably occurs with histidine as well. van Heyningen has found free fluorescent substances in human lenses which can sensitize the photooxidation of lens

protein and appear to be derived from tryptophan metabolism. Pirie's research indicates that the brown insoluble protein in cataractous human lenses may be linked to the lens proteins and appear to be derived from tryptophan metabolism. Pirie's research indicates that the brown insoluble protein in cataractous human lenses may be linked to the lens proteins by fluorescent pigmented photoproducts. Kurzel, Wolbarsht, and Yamanashi[28, 29] have presented evidence that tryptophan photoproducts were bound to human cataractous lens proteins by fluorescence and phosphorescence studies of the whole lens. Although products of tryptophan were identified, it was not clear whether these products were bound or a part of the peptide chain.

Zigman et al[30] studied the chemical effects of near UV radiant exposure on tryptophan using human crystalline lenses. The source was a photochemical lamp filtered to produce a wavelength range from 340 nm to 380 nm with an irradiance of 3.0 $mWcm^{-2}$ and a maximum emission at 365 nm. They found that exposure of tryptophan to near UV leads to chromatic photoproducts which bind to the lens proteins, alter their color and change solubility. Human lens materials without added tryptophan did not show chromatic changes on exposure to long-wavelength UV until after 48 hours of exposure. Tryptophan showed an excitation wavelength at 278 nm and a fluorescent emission at 330 nm. However, following exposure to near ultraviolet, tryptophan showed an additional 360 nm excitation and 440 nm fluorescence similar to that found in the brunescent human cataract lenses.[31] The ultraviolet irradiance for these studies was 3 to 5 $mWcm^{-2}$ at 365 nm and exposures were made for at least several hours. These exposure levels exceed those expected for sunlight in the same wavelength range for the same period of time.

Zigman et al[32] and Zigman and Vaughan[33] have continued research in the above area and have shown mouse eye tissue damage for exposures of 12 hours a day up to 90 weeks. Lens epithelial cells seemed to lose their ability to differentiate into fiber cells after 35 weeks of exposure while anterior and posterior cataracts developed at 50 weeks. The retinal photoreceptors of these mice became thin, then were invaded by phagocytic wandering cells and destroyed. Photoreceptor thinning was noted by 14 weeks and total loss of the photoreceptors occurred by 70 weeks. No corneal damage was observed. Zigman and Bagley[34] in an in vitro study of dogfish retinas have shown that RNA and protein precursor incorportion in the photoreceptors was inhibited after exposure to 3 to 4 $mWcm^{-2}$ at 365 nm for 8 hours. They suggested that the mechanism was an inhibition of cytochrome activity which had been shown previously to be sensitive to blue and near UV exposure.

In an attempt to determine the role of near UV in the production of cataracts, Zigman et al[35] studied in vitro dogfish lenses and mice exposed to a near UV environment. Freshly enucleated dogfish lenses were prepared and incubated with a 320 to380 nm bandwidth ultraviolet source with an irradiance of 3.0 $mWcm^{-2}$ for 24 hours prior to biochemical evaluation. The mice were reared in a controlled near UV environment

which ranged in irradiance from 200 $\mu W cm^{-2}$ to 600 $\mu W cm^{-2}$ with a peak wavelength at 365 nm. At 6 to 7-week intervals, the mice were sacrificed for histologic and biochemical study. The mouse research showed that the in vivo effect of near UV was to inhibit the accumulation of soluble proteins in the lens. This could have resulted from a direct effect on the protein-synthesizing system or from the direct blockage of amino acid uptake as a result of lens capsule and fiber alterations. The mouse lenses also showed a marked increase in insoluble protein between 16 weeks and 43 weeks. Thus, it appears that near UV accelerates the aging process in mice by changing soluble crystallines into insoluble crystallines.

Zigman et al's[36] data show that there are at least two methods in which near UV exposure may alter the physical and chemical properties of the crystalline lens. Free aromatic amino acids may be photooxidized into compounds with strong binding affinities for lens proteins. Near UV may also photooxidize these same aromatic amino acids that comprise the protein. In either case, the photooxidation from near UV causes an increase in a yellow-brown coloration of the lens material. The photooxidation process is inhibited by the presence of ascorbic acid.

Although many investigators support the thesis that the brown or brunescent nuclear cataract results from solar photooxidation of the lens protein,[13, 14, 17, 18, 19, 37] the concept has not been experimentally proven. Harding and Dilley[38] provide two major arguments against this hypothesis:

> "(1) In brown nuclear cataract it is only the nucleus that is pigmented but any ultraviolet light reaching the lens will be absorbed by and, therefore, act on the proteins at the front of the lens. If proteins from the separated cortex and nucleus of the normal human lens are photooxidized in vitro, both go brown and at precisely the same rate.[39]
>
> (2) Photooxidization of lens protein in vitro by sunlight destroys tryptophan[40] but the proteins of the brown cataractous nucleus have as much tryptophan as those of the normal human lens,[39] contrary to an earlier report."

Extrapolations from experimental animal data to humans must be qualified. Human cataractous lenses do show increased insoluble proteins and/or the presence of brown pigmented material with many of the same characteristics as the tryptophan photoproducts. Additionally, the human lens does absorb most of the near UV radiation striking the eye at an appropriate angle. UV induced cataracts have been experimentally produced in mice, rabbits, monkeys, and guinea pigs, and after both single and multiple daily exposures over a wide range of UV irradiances. Thus, UV is implicated as a potential cause of cataracts in humans.

Ultraviolet Effects in the Presence of Photosensitizing Drugs

Dramatic increases in the sensitivity of skin to the near ultraviolet and other wavebands are induced by a variety of pharmaceutical compounds. The most potent near UV photosensitizing compounds known for skin are certain furocoumarins called psoralens. Some experimental animals studies indicate that 8-methoxypsoralen, one of the more phototoxic psoralens when applied to skin or taken orally, also sensitizes the eyes of certain species to near UV exposure. It is not yet known how this relates to the use of psoralens in photochemotherapy of humans.

Griffin[41] examined the erythemal and carcinogenic response associated with oral (dietary, 0.5 g/kg diet) and intraperitoneal (0.4 mg/mouse/day, one hour before UV exposure) administration of methoxsalen and subsequent exposure of albino mice to ultraviolet radiation greater than 320 nm. The mice were irradiated daily for a period of six to twelve weeks.

Cloud et al[42] found that 80 mg/kg of 8-methoxypsoralen fed to guinea pigs sensitized the ocular tissues to damage by subsequent exposure to "black light". The skin of the eyelid was eroded and the cornea was edematous. Anterior cortical lenticular opacities developed within 5 months after a 24-hour exposure and were the only significant observed changes after a chronic exposure of 10 minutes a day for 6 days a week for up to 5 months duration. Cloud et al do not provide the radiant emittance of the source and were interested only in the gross changes since histologic observations were not reported.

Cloud et al[43] performed another experiment in which albino mice received 10 minutes a day of UV exposure one hour after intraperitoneal injection of 4 mg (160 mg/kg) of 8-methoxypsoralen. The animals received the drug and were exposed to light six days a week for five months and were observed for an additional five months. The radiation source was Sylvania (BLB) black light blur tubes that emitted strongly between 320 and 400 nm. The irradiance was not given. Reactions in the mice were severe. Fifty percent of the mice receiving 8-methoxypsoralen died, whereas 13% of the controls not receiving the drug died. The ears of all mice receiving psoralen plus near UV had damage which ranged from shriveling of the edges of the ear to the loss of the entire external ear. A typical leukoma, with or without vascularization and punctate keratitis, were found in the cornea. Eighty-nine percent of the 28 mice that lived 10 weeks developed cataracts, 64% of which were anterior cortical cataracts. There is no doubt that at the extreme drug doses given, 8-methoxypsoralen increased damage in the mice.

Freeman and Troll[44] investigated the action spectrum for eye damage in guinea pigs receiving oral 8-methoxypsoralen (88 mg/kg). The animals' eyes were exposed to various single exposure doses of 5 nm half-bandwidth radiation from a xenon arc and grating monochromator system. Exposures were given one hour after oral administration of the 8-methoxypsoralen, and at 10 nm spectral intervals from 300 to 390 nm. The animals were observed for evidence of eye injury for 72 hours after irradiation. Special attention was given to corneal injury, clouding of the anterior chamber, and conjunctival hyperemia. The maximum efficiency of photosensitization of the eyes was found between 320 and 340 nm. No apparent damage from 8-

methoxypsoralen was found at wavelengths longer than 380 nm. They also found that guinea pigs were more susceptible to photosensitizing injury with psoralens and near UV than were rabbits.

When guinea pigs were given repeated doses of 8-methoxypsoralen and exposed to near UV radiation comparable to photochemotherapeutic doses for man, no eye damage was detected.[44] 8-methoxypsoralen was administered intraperitoneally (0.5 mg/kg) to albino guinea pigs daily for 13 months. Animals were exposed daily to 10 hours of fluorescent near UV, (F40 BLB) lamps, at a distance of 10 inches. This long-term study revealed no gross, ophthalmoscopic, slit lamp, or histologic manifestations of ocular injury. This suggests that the ocular photosensitizing effects of 8-methoxypsoralen may therefore be limited to single exposures above some threshold value.

Egyed et al[45] fed 16 two-to-three-week-old ducklings the seeds of Ammi majus, the plant from which 8-methoxypsoralen is extracted. The animals were exposed to the sun for four to five hours per day. Acute conjunctivitis was observed in two to three days. The animals developed mydriasis (dilation of pupils) and severe pigmentary retinopathy after one month. No cataracts were observed. A control group of ducklings exposed to the sun but without the ingestion of plant seeds containing 8-methoxypsoralen showed relatively few ocular changes. Twenty percent of the control ducklings showed areas of retinal hyperpigmentation similar to those which developed in the experimental animals of the study. However, in the control group these areas were less dense than in the seed-treated group. Egyed's work has been recently confirmed by that of Barishak et al[46], who reported pigmentary retinopathy and histologic changes of the choroid in ducklings photosensitized by force-feeding of Ammi majus seeds and subsequent exposure to sunlight.

Evidence of ocular photosensitization in humans by psoralens is lacking, although these drugs in combination with sun exposure have a long history of use in folk medicine and in dermatologic practice. The relatively recent isolation and use of 8-methoxypsoralen in photochemotherapy merits a thorough following of possible ocular effects in these patients. The patient's eyes are protected during photochemotherapy treatment, but some small near UV exposure to the eye is unavoidable during the approximately eight-hour period of sensitization after ingestion of 8-methoxypsoralen.[47]

Ultraviolet Laser Radiation Effects

Ultraviolet lasers have recently been used to produce corneal and lenticular damage. MacKeen, Fine, and Fine[48] exposed weanling rabbits to a He-Cd laser operating at 325 nm with a power output of 15 W and a 1.5-mm beam diameter. The power density was 0.85 Wcm^{-2} with exposure durations of 4, 6, 8, 16 or 32 minutes. The initial response observed was an edema of the corneal epithelium which occurred within the first few hours and was reversible. All 32-minute-duration exposures (about 1632 Jcm^{-2}) showed localized anterior sub-capsular changes after three days which did not spread laterally

with age. The final appearance was a division of the initial sub-capsular opacity into a large anterior cortical opacity and a small sub-capsular cataract. Adult rabbits of 9 to 11 kg body weight developed deep anterior cortical cataractous changes after a period of 6 months.

Ebbers and Sears[49] used a He-Cd UV laser and exposed 100 monkey eyes. The endpoint for corneal damage was a well-defined corneal lesion. An ED_{50} of 0.8 Jcm^{-2} was established and the corneal damage completely reversible within 24 to 48 hours. Ebbers and Sears reported that permanent lenticular cataracts were produced with a 6.5 Jcm^{-2} radiant exposure.

Zuclich and Connolly[50] reported on corneal and lenticular damage from a kryptonion laser with continuous wave (cw) output at 350.7 nm and 356.4 nm simultaneously with an intensity ratio of ≃3:1, an argon-ion laser with cw output at 351.1 nm and 363.8 nm simultaneously with an intensity ratio of ≃1:1 and a nitrogen laser emitting at 337.1 nm with a 10 ns pulsewidth and a variable repetition rate up to 50 Hz. The nitrogen laser had a peak power of ≃1 megawatt. The krypton-ion laser (350.7 nm and 356.4 nm) produced corneal epithelial lesions in rhesus monkeys with a radiant exposure of approximately 70 $Jcm.^{-2}$ The lesions developed within 12 to 24 hours and the epithelium regenerated back to normal within 48 hours. Multiple exposures with pulse-widths varying from 250 ns to 1 s and a pulse train of 30 s resulted in corneal damage threshold of 67 $Jcm.^{-2}$ The nitrogen laser (337.1 nm) gave a corneal radiant exposure threshold of $8.4^{\pm}$ $Jcm.^{-2}$ Lenticular clouding was produced with a single 10 ns pulse with nitrogen laser radiant exposure of 1.1 $Jcm.^{-2}$ Immediate visible cataracts were found with two or more pulses. The threshold for lenticular cataracts with the argon-ion laser was 76 Jcm^{-2} for a 4 s exposure with a power output of 1 watt. The corneal irradiance for that exposure was 19 $Wcm.^{-2}$ One second exposures produced a lenticular opacity with a radiant exposure threshold of $19^{\pm}$ 1.8 $Jcm.^{-2}$ Retinal damage was reported with the krypton and argon laser but threshold determinations could not be made because of the variability between animals. Zuclich and Connolly concluded that the corneal damage was photochemical because the reciprocity relationship between pulsewidth and exposure threshold was equivalent to 67 Jcm^{-2}. However, lenticular damage did not follow the reciprocity relationship and was postulated to be thermal.

In another paper, Zuclich and Kurtin[51] demonstrated that corneal damage induced by argon-ion laser (351 nm and 363 nm) in rhesus monkeys is somewhat oxygen-dependent. The authors obtained average corneal damage thresholds of 82 J/cm^2 in air, 66 J/cm^2 after the eyes have been exposed to 0_2 for 15 minutes prior to exposure, and 133 J/cm^2 after exposure of the eyes to 15 minutes of N_2. This is taken by the authors as evidence of a photodynamic effect of UV on corneal tissue. When exposure duration was varied,

the threshold irradiance correspondingly changed in such a way that the total energy dose remained relatively constant and the effects of repetitive exposures were cumulative. These observations were felt to indicate that corneal damage was initiated by a single photon photochemical process.

The recent data of Ham et al[52] in rhesus monkeys clearly demonstrates markedly increased retinal damage by exposure to the shorter visible wavelengths. Blue laser radiation caused retinal lesions in the monkeys at approximately 1/1000 the irradiance necessary to produce thermally-induced retinal lesions using red laser radiation. The action spectrum for such retinal lesions may include the UV region around 400 nm. There is no reason to believe that UV could not photochemically or thermally induce retinal lesions if the ocular spectral transmission of the species in question allows the near ultraviolet to reach the retina.

Summary of Near Ultraviolet Research

Experimental exposures of animals and humans indicate that for wavelengths shorter than approximately 290 nm, keratitis and alterations of the cornea are the major ocular hazards. These reactions and effects are usually painful but reversible. UV-induced alteration of the cornea appears to follow a photochemical mechanism.

At ultraviolet wavelengths longer than 290 nm, radiation may reach the lens, iris, aqueous humor, and the retina. Experimental evidence in rabbits and monkeys indicates that permanent lenticular cataracts may be produced by single, high irradiance (Laser) or long exposure durations (high-pressure arc lamps) to ultraviolet radiation above 290 nm. This observed damage may be induced by thermal and/or photochemical mechanisms in the lens. Cataracts have been produced in albino mice with mulitple UV exposures below the single threshold exposure level for ocular damage. Ultraviolet induced cataracts in humans have not been proved by controlled scientific experiments in spite of the fact that some epidemiologic studies[53] suggest that human cataracts may be related to solar exposure and, hence, UV exposure. Extrapolation of animal cataract data to the human may be highly uncertain especially since the mechanism for UV induced cataracts in animals has not been established.

Biochemical studies in human and animal lenses indicate that the near UV may induce lenticular cataracts by an alteration of lens crystalline proteins from lower molecular weight soluble proteins to higher molecular weight insoluble proteins. It is clear that definitive evidence for the involvement of the near UV in the development of the human brunescent cataract is lacking. It is conceivable that a well planned study on the mechanisms of UV induced cataracts using an animal model may provide the information needed to understand the causes of radiation cataracts specifically and other cataracts in general.

Increased ocular damage is observed following near UV exposures of experimental animals who have been administered 8-methoxypsoralen. The mechanism of ocular photosensitization by 8-methoxypsoralen is not certain and needs further investigation. An attempt to mimic the doses of 8-methoxypsoralen and near UV employed in photo-

chemotherapy of humans produced no observable ocular changes in guinea pigs after daily treatment for 13 months. Evidence of potential ocular hazards of oral psoralens plus near UV in humans is lacking. The need for verification and elucidation of the ocular effects produced by UV alone and by UV in combination with photosensitizing drugs should be apparent.

INSTRUMENTATION AND PROCEDURES

Ultraviolet Source

The source for the ultraviolet energy was a 5000 watt xenon-mercury high pressure lamp, powered by a 10 kW, DC power supply regulated to ±0.5% and capable of delivering from 0 to 80 amperes at 25 to 65 volts to the arc electrodes (Figure 9). The lamp housing was cooled by two blowers. Adequate cooling was available except when the lamp was operated at maximum amperages.

The radiation from the source (Figure 9) was focused at the monochromator entrance slit by the housing optics. A 10-cm quartz enclosed water chamber was placed between the focusing lenses and the monochromator to remove the infrared radiation. The desired UV wavebands were obtained with a Model 25-100 Jarrell-Ash Czerny Turner double grating monochromator or a McPherson Model 2051 single grating monochromator.

The Jarrell-Ash monochromator gratings were blazed at 300 nm with 1180 grooves per millimeter, and a linear dispersion of 0.82 nanometers per millimeter. The entrance, intermediate and exit slits were set to pass a full-bandwidth of 6.6 nm; however, all wavebands are reported as 5.0 nm. Stray light could not be measured through the system.

The McPherson monochromator grating was blazed at 300 nm, with 300 grooves per millimeter, and a 3.3 nanometer per millimeter linear dispersion. The entrance and exit slits were set to provide a 9.96 nanometer full-bandwidth wavelength. All wavebands are reported as 10.0 nm. The stray light was measured to be less than 0.2%; therefore, stray light will be ignored in the evaluation of radiant exposures since that amount is negligible.

The monochromator systems were aligned with a Helium-neon laser and the wavelength counter calibrated with a mercury source. Exposure durations were set with an H-P Model 5330B preset counter which controlled a Gerbands electronic shutter. The shutter system allowed the control of exposure durations to any desired length with millisecond accuracy.

Ultraviolet Source Measurement

An EG&G 580/585 radiometer was used to calibrate the UV source. The EG&G radiometer was cross-calibrated against an Eppley 16-junction thermopile traceable to an NBS UV standard source (Figure 10). The radiometer was placed in the same position that the animal's cornea would occupy during exposures.

The irradiance in Wcm^{-2} incident on the radiometer was determined by the following relationships:

$$E_{e\lambda} = \frac{I_m M_d}{K_\lambda} \qquad (1)$$

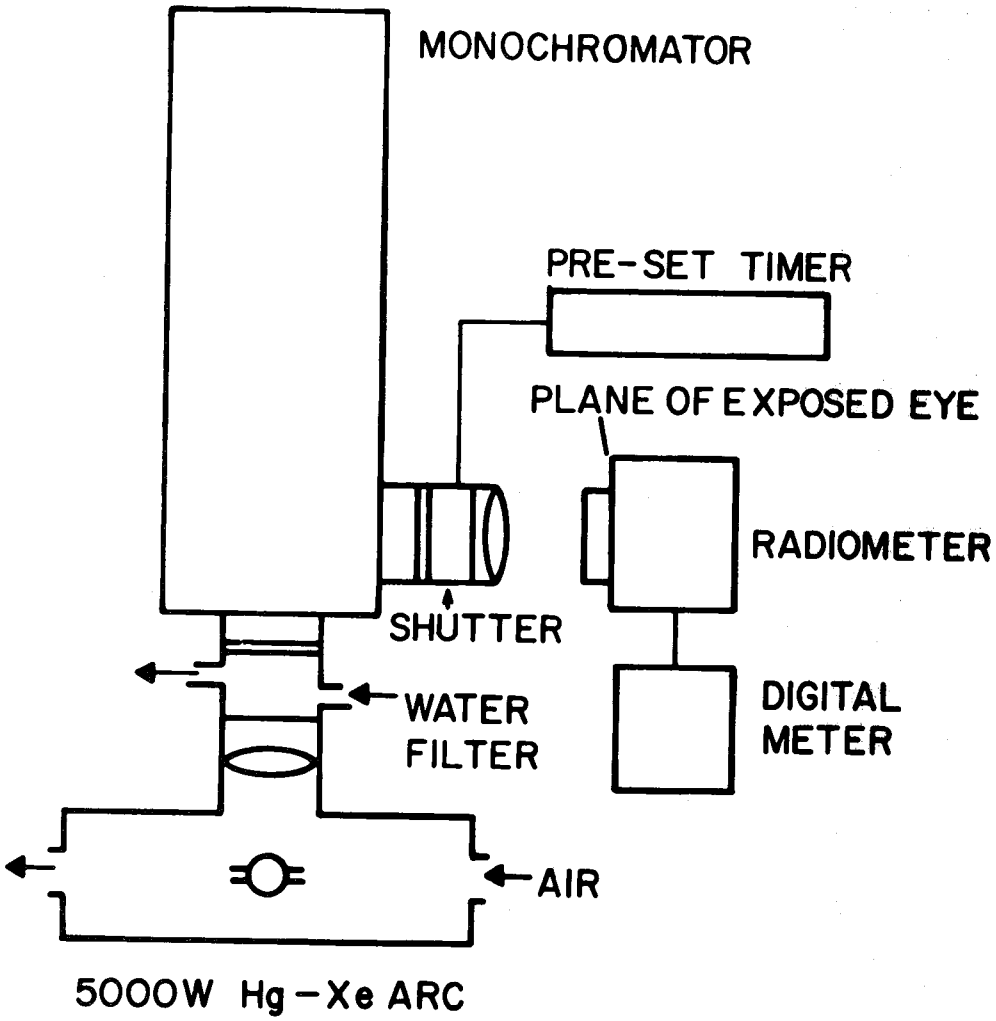

Figure 9: Schematic of the exposure instrumentation. See text for detailed description of the system, calibration techniques and exposure procedures.

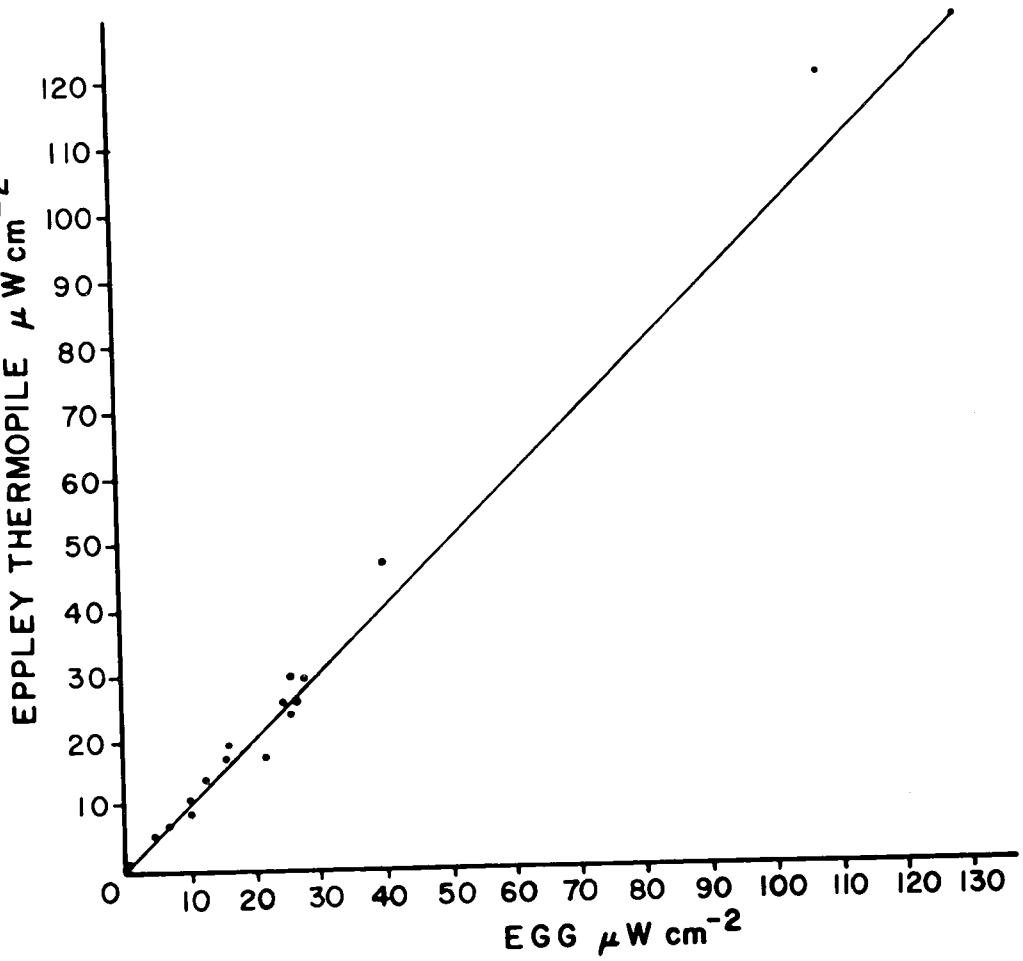

Figure 10: Cross calibration of the EG&G radiometer against the Eppley thermopile using the NBS standard 1000 W tungsten filament, quartz-iodine lamp.

$E_{e\lambda}$ = irradiance in Wcm^{-2} for the waveband of concern

I_m = current or ampere reading from the radiometer

M_d = multiplying aperture

K_λ = radiometer calibration constant

Equation (1) was valid for the measurement of sources having a diameter equal to or larger than the aperture of the radiometer.

The radiant exposure (H) in Joules/cm^2 (Jcm^{-2}) was calculated using the following:

$H = E_{d\lambda}\, t$

H = radiant exposure (Jcm^{-2}) (2)

$E_{e\lambda}$ = irradiance (Wcm^{-2})

t = exposure duration in seconds

For a given irradiance $E_{e\lambda}$, the exposure duration t could be varied to obtain different values for the radiant exposure H. The exposure duration t, irradiance $E_{e\lambda}$, and radiant exposure H were determined for each animal prior to exposure using the above calibration procedure. The calibration accuracy was estimated to be approximately +10%. The spectral irradiance of the source using the double monochromator and the EG&G radiometer is shown in Figure 11.

Experimental Animals

Normal healthy, pigmented rabbits, 2 to 3 kg. in weight, were the experimental animals. The animals were used in experiments without regard to sex. The animals were housed in quarters under controlled, normal lighting conditions. All animals were procured from a single source to insure constant breeding practice. Nine primate eyes (Galago senegalensis) were exposed to provide additional information.

There were several reasons for the selection of the pigmented rabbit. Foremost was the fact that almost all previous research on the effects of ultraviolet radiation on the eye had used the rabbit and continued use of the rabbit would allow comparison of the data with other research. The anatomy of the rabbit's eye is well known and the differences in the anterior structure of the rabbit eye from the human eye are minimal and well established. Finally, the rabbit is small, easily handled, reasonably inexpensive, and can be readily examined with the biomicroscope and ophthalmoscope without the use of anesthetics.

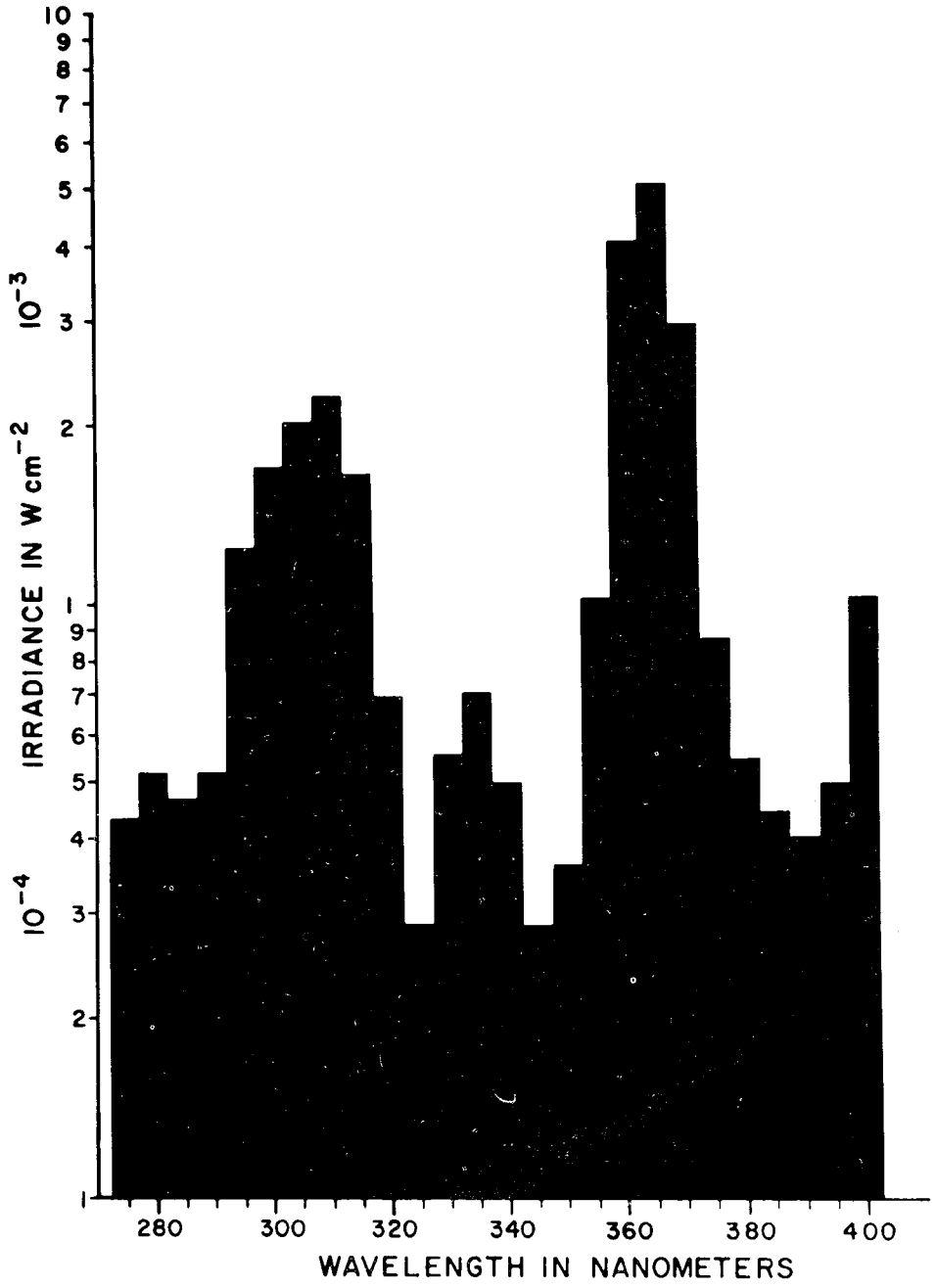

Figure 11: Spectral irradiance of the 5000 W Xe-Hg high pressure lamp using the double monochromator and the EG&G radiometer for 5 nm wavebands.

All animals were placed in a specially designed rabbit holder for exposure sessions and biomicroscopic examination.

Evaluation and Exposure Procedures

Prior to exposure, each eye was examined thoroughly with the biomicroscope. Any animal with anomalies of the anterior part of the eye (cornea, anterior chamber, iris, or lens) was rejected. The cornea was centered normal to the optical beam with the monochromator set at 450 nm. The eyes were exposed in 5 nm or 10 nm waveband steps in the wavelength range from 290 nm to 400 nm.

Exposures at particular wavelengths were discontinued if the source irradiance were not sufficiently high to produce corneal or lenticular damage in an 8 hour exposure (28,800 seconds). This procedure was adopted in an attempt to limit laboratory exposures to durations equivalent to a normal work period for humans. Exceptions were made when the wavelength was of particular interest; for example, wavelengths 325 nm and 365 nm were considered important in establishing lenticular damage. These exceptions were dictated by the spectrum and the spectral irradiance of the source. An additional quartz lens was added to the optical system to reduce the size of the optical beam and increase the irradiance per unit area of the beam. Exploratory exposures showed greatly increased variability of the data because ocular movements did not allow the optical beam to remain on same area off the cornea and the lens during exposure.

Ocular damage criteria are given in Table I. The criteria used to determine corneal damage were epithelial debris, epithelial stippling, epithelial granules, epithelial haze, epithelial exfoliation, stromal haze, stromal opacities, and endothelial disturbances. Anterior chamber signs included flare and cells. The crystalline lens criteria were sub-capsular opacities, capsular and stromal haze, stromal opacities, and increased prominance of the anterior suture. Criteria for the iris were the presence of the anterior chamber signs, changes in clarity of the iris stroma, and a sluggish pupillary response.

Epithelial debris may be described as small glistening bodies located in the pre-corneal tear layer. Epithelial haze is an irregular, crackled appearance of the corneal anterior surface. Epithelial granules are small, white, discrete, round spots located deep in the epithelial layer of the cornea. Epithelial exfoliation is a sloughing of layers of the epithelium. Stromal haze is a loss in the transparency or an increased scatter of the biomicroscope light from the stroma. Stromal opacities are localized areas of opacification. Endothelial disturbances include granular formations similar to the epithelial granules and keratic precipitates (KP's). Anterior chamber flare is the Tyndall scatter produced by the release of non-cellular blood components into the aqueous of the anterior chamber. Anterior chamber cells are the release of cellular materials into the aqueous. Sub-capsular opacities are small, discrete white dots located in the anterior epithelium just beneath the capsule of the lens. Capsular and stromal haze are the result of increased scatter of the lens capsule and stroma. Stromal opacities appear to be migrations and coalescing of the sub-capsular opacities into "clumps".

TABLE I OCULAR ULTRAVIOLET DAMAGE CRITERIA

1. Cornea

   A. Epithelium

      Discharge
      Epithelial Debris
      Epithelial Haze
      Granules
      Exfoliation

   B. Stroma

      Stromal Haze
      Stromal Opacities

   C. Endothelial Disturbance

2. Anterior Chamber

   Flare
   Cells

3. Lens

   Capsule
   Cortex
   Nucleus

4. Iris

   Stromal Haze
   Pupillary Reaction
   Posterior Synechia

Two observers independently determined the criteria status and classification of each eye. The severity of the exposure for the corneal criteria was indicated as negative (-), probably positive but not certain ($\pm$), positive (+), moderately positive (++), severely positive (+++), and extremely positive (++++). If five or more corneal criteria were positive (+), the eye was classified as above threshold (+). Three to four positive corneal criteria were classified as threshold ($\pm$). Fewer than three positive corneal criteria resulted in a below threshold classification (-). Any lens or anterior chamber signs resulted in a positive (+) classification.

The lowest radiant exposure resulting in an above threshold classification terminated the experiment for that waveband.

Conventional statistical rounding procedures were used. All data was rounded to three significant figures. Each experimental session covered approximately 14 hours.

Procedures for Electron Microscopy

The eye was removed and immersed in fixative for 60 s to permit the cornea to be fixed while under pressure from the aqueous. The eye was then bisected posteriorly, the lens subluxated, and all of the tissues were fixed for 30 minutes. In those circumstances where the lens was to be preferentially fixed, it was subluxated immediately after the eye was enucleated and bisected. Three fixatives were used: a modification of Karnovsky's fixative (1965), a 3-4% gluteraldehyde solution and a mixture of 3-4% gluteraldehyde, 2% aqueous osmium tetroxide and a 1% ruthenium red solution in a 1:1:1 ratio. The fixed eyes were kept in holding solutions in the refrigerator until dissected. The cornea was slivered and only the anterior portion of the lens including the capsule, anterior epithelium, and anterior cortex was dissected.

The tissues were dehydrated in a graded ethanol series followed by rinses in propylene oxide and embedded in epoxy resin, araldite or Spurr's medium. They were sectioned on a Sorvall MT-2 ultramicrotome and viewed with a JEOL 100C electron microscope.

RESULTS

Ultraviolet exposures were made on 158 pigmented rabbit eyes and 9 primate eyes (Galago senegalensis) during the course of this investigation. In addition, thirty-five eyes were exposed for electron microscopic study. The data will be presented in tabular form, graphic form and discussion form based on the biomicroscopic and electron microscopic findings. The 5-nm full-waveband and 10-nm full-waveband data have been combined for the results presentation. This was felt justified because exposures made at 300 nm with each waveband resulted in almost identical results. The differences between the 5-nm waveband exposures and 10-nm waveband exposures were within the measurement error of the source.

Table II presents the rabbit and primate exposure data including the wavelength, animal number, animal eye, irradiance, exposure duration, radiant exposure, the biomicroscopically determined classification for the radiant exposures, and the threshold radiant exposure values for the cornea H_C and the lens H_L. The threshold radiant exposure values for the cornea H_C and lens H_L are presented in Table III and Figure 12. Figure 13 compares the ultraviolet action spectrum for the human primate and rabbit[54-59] with the corneal and lenticular thresholds generated in this investigation.

In Figure 12, the cornea and lens curves are relatively parallel up to about 320 nm where a separation occurs as the result of the dramatic increase in the lenticular threshold. It appears that the action spectrum for corneal threshold extends to about 310 nm. Above 310 nm, there is a sudden rise in the radiant exposure threshold for the cornea. The action spectrum for the lens begins at about 295 nm and extends to 320 nm in which relatively low radiant exposures were required to produce lenticular opacities. The cornea would be damaged at lower radiant exposures and should provide protection against lenticular damage.

Figure 13 compares corneal and lenticular damage in the 290 nm to 400 nm wavelength range to the previous corneal data of Pitts et. al.[54-59] for the rabbit, primate and human corneal thresholds. Limited data above 300 nm for the human eye does not allow a detailed comparison; however, the human corneal threshold was considerably below that for either the rabbit or the primate. The primate corneal threshold was somewhat below the rabbit corneal threshold until 320 nm where little or no difference was found. The sharp rise in the lens threshold below 300 nm is probably due to the absorption characteristics of the cornea (Figure 8). Almost complete absorption of the ultraviolet radiaton occurs at 290 nm and below. The radiant exposure required to produce a threshold response at 290 nm was at least 20 times the threshold value at 300 nm (3.0 Jcm^{-2} vs. 0.15 Jcm^{-2}) and supports establishing the lower wavelength of the lens action spectrum at 295 nm.

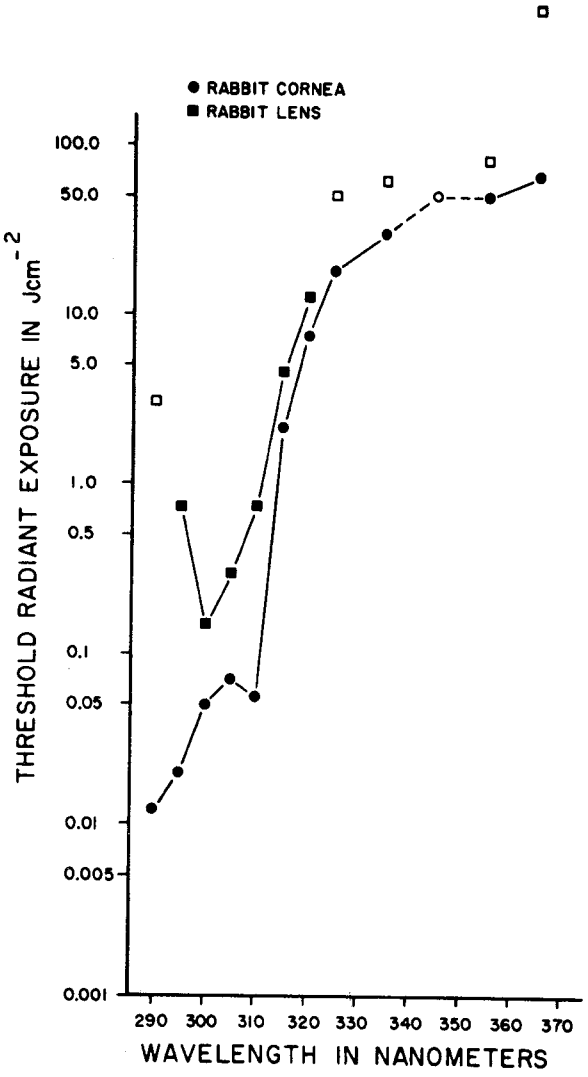

Figure 12: Radiant exposure for corneal and lenticular thresholds. The open squares represent the highest radiant exposure attained during this study. No lenticular damage was produced at these exposure levels. The open circle represents a single exposure at 345 nm which was judged to be corneal threshold. The data points refer to a wavelength band rather than discrete wavelengths.

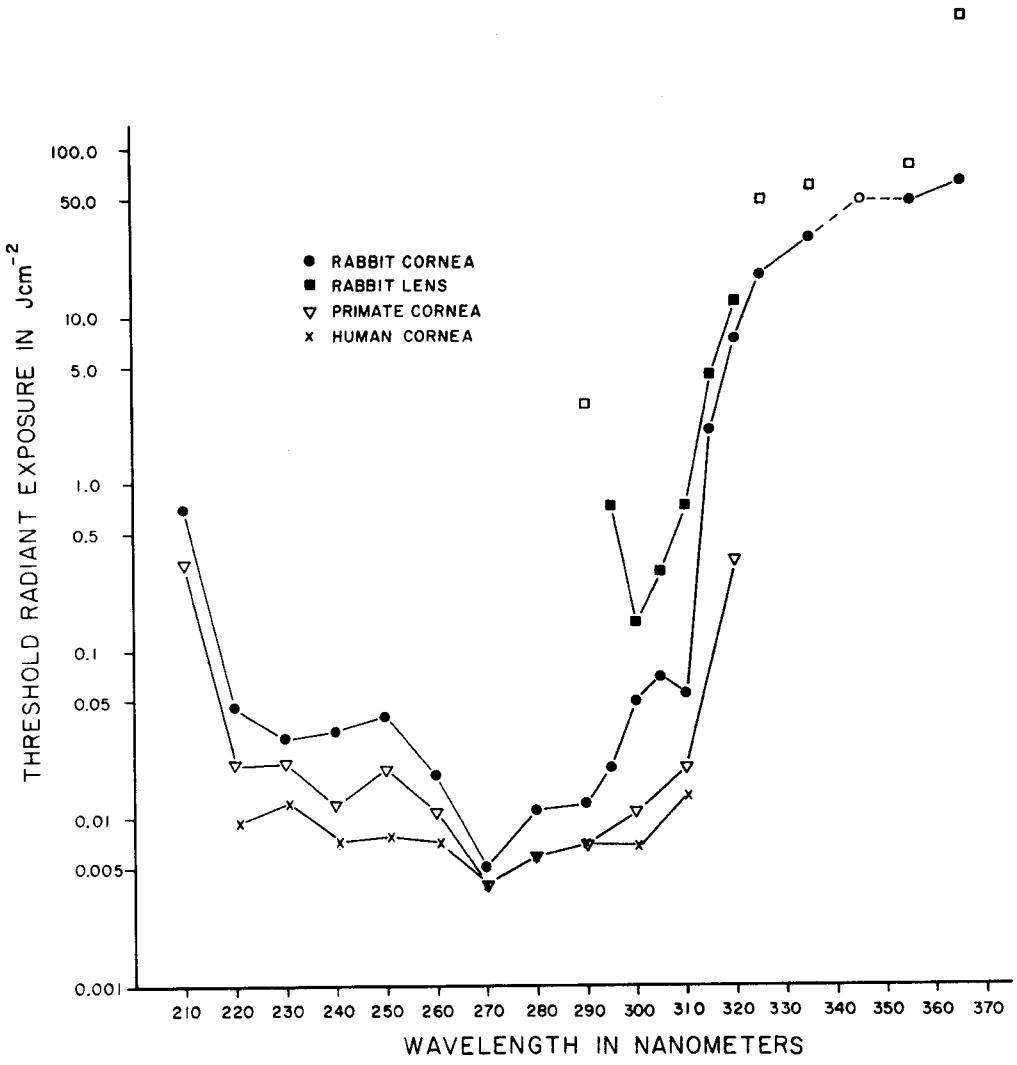

Figure 13: Comparison of the corneal and lenticular thresholds with previous rabbit, primate, and human thresholds.[55,57] The open squares represent the highest radiant exposures attained during this study. No lenticular damage was produced at these exposure levels. The open circle represents a single exposure at 345 nm which was judged to be corneal threshold. The data points refer to a wavelength band rather than to discrete wavelengths.

TABLE II EXPOSURE DATA

Animal Number	Irradiance $Wcm^{-2}x10^{-3}$	Exposure Duration(s)	Radiant Exposure Jcm^{-2}	Classification Cornea / Lens	
PIGMENTED RABBIT EXPOSURES					
			Waveband 290 nm		
			5-nm Bandwidth Exposures		
			0.012	* H_C	-
H0130L	0.853	8,486	0.724	+++	-
H0146R	0.128	24,348	3.116	++++	-
			Waveband 295 nm		
			5-nm Bandwidth Exposures		
H08R	0.055	254.	0.014	-	-
H07R	0.055	290.	0.016	-	-
H03R	0.153	105.	0.016	-	-
H05R	0.055	326.	0.018	-	-
H04L	3.478	5.18	0.018	-	-
H02R	0.159	118.	0.019	$\pm$	-
H01R	0.153	130.	0.020	H_C	-
H02L	3.478	6.32	0.022	+	-
H03L	3.478	7.19	0.025	+	-
H01L	3.478	7.48	0.026	+	-
H07L	0.067	496.	0.033	+	-

* Determined in previous study.[54]

TABLE II EXPOSURE DATA cont.

Animal Number	Irradiance $Wcm^{-2}x10^{-3}$	Exposure Duration(s)	Radiant Exposure Jcm^{-2}	Classification Cornea / Lens	
		5-nm Bandwidth Exposures (cont'd)			
H094R	0.093	5400.	0.500	+++	-
H097R	0.102	7339.	0.750	++++	H_L
H070R	0.124	8064.	1.000	++++	+
		Waveband 300 nm			
		5-nm Bandwidth Exposures			
H0107R	0.199	101.	0.020	-	-
H0105R	0.199	126.	0.025	-	-
H0108R	0.199	151.	0.030	-	-
H010L	0.197	167.	0.033	- to $\pm$	-
H0106L	0.199	205.	0.041	- to $\pm$	-
H0111L	0.366	137.	0.050	H_C	-
H0110R	0.366	164.	0.060	+	-
H0109R	0.366	191.	0.070	+	-
H0112R	0.366	219.	0.080	++	-
H096R	0.241	414.	0.099	+++	-
H092R	0.227	441.	0.100	+++	-
H093R	0.227	661.	0.150	+++	H_L
H090R	0.241	828.	0.200	++++	+
H089R	0.241	1242.	0.300	++++	+

TABLE II EXPOSURE DATA cont.

Animal Number	Irradiance $Wcm^{-2}x10^{-3}$	Exposure Duration(s)	Radiant Exposure Jcm^{-2}	Classification Cornea / Lens	
		5-nm Bandwidth Exposures (cont'd)			
H091R	0.241	1657.	0.400	++++	+
H085L	0.268	1866.	0.500	++++	+
		10-nm Bandwidth Exposures			
H0227L	3.834	14.0	0.054	H_C	-
H0226R	3.834	22.0	0.084	++	-
H0220R	3.834	40.0	0.153	+++	H_L
H0224L	3.834	80.0	0.306	++++	+
		Waveband 305 nm			
		5-nm Bandwidth Exposures			
H023R	0.298	124.	0.037	-	-
H020R	0.310	129.	0.040	-	-
H016L	0.307	153.	0.047	-	-
H0117R	0.385	130.	0.050	-	-
H025R	0.307	163.	0.050	$\pm$	-
H06L	0.273	183.	0.050	$\pm$	-
H010R	0.268	231.	0.053	$\pm$	-
H08R	0.314	191.	0.059	$\pm$	-
H0123R	0.385	156.	0.060	- to $\pm$	-
H07R	0.314	223.	0.069	$\pm$ to +	-

TABLE II EXPOSURE DATA cont.

Animal Number	Irradiance $Wcm^{-2}x10^{-3}$	Exposure Duration(s)	Radiant Exposure Jcm^{-2}	Classification Cornea	Classification Lens
		5-nm Bandwidth Exposures (cont'd)			
H0126L	0.385	182.	0.070	H_C	-
H012R	0.332	225.	0.075	+	-
H086R	0.341	293.	0.100	++	-
H0114L	0.406	493.	0.200	+	-
H088R	0.341	880.	0.300	+++	H_L
H0116L	0.406	986.	0.400	+++	+
H080R	0.327	1528.	0.500	++++	+
H067R	0.327	3055.	0.999	++++	+
H077R	0.327	4583.	1.500	++++	+
		Waveband 310 nm			
		5-nm Bandwidth Exposures			
H0102R	0.153	261.	0.040	-	-
H012L	0.126	398.	0.050	-	-
H0125R	0.274	201.	0.055	H_C	-
H0104R	0.153	391.	0.060	+	-
H013R	0.133	564.	0.075	+	-
H0AL	0.248	2018.	0.500	++	-
H0101R	0.153	4892.	0.750	++	H_L
H0128L	0.289	2780.	0.801	++	+

TABLE II EXPOSURE DATA cont.

Animal Number	Irradiance $Wcm^{-2}x10^{-3}$	Exposure Duration(s)	Radiant Exposure Jcm^{-2}	Classification Cornea / Lens	
		5-nm Bandwidth Exposures (cont'd)			
H0115R	0.277	3247.	0.900	+++	+
H0BL	0.248	4036.	1.000	+++	+
H0CR	0.248	6053.	1.500	++++	+
		Waveband 315 nm			
		5-nm Bandwidth Exposures			
H022R	0.551	90.	0.049	-	-
H021L	0.551	109.	0.060	-	-
H029L	0.553	118.	0.065	-	-
H030L	0.553	127.	0.070	-	-
H06L	0.589	127.	0.075	-	-
H023R	0.578	135.	0.078	-	-
H033R	0.550	164.	0.090	-	-
H034R	0.550	182.	0.100	-	-
H036R	0.550	200.	0.110	-	-
H037R	0.595	1681.	1.000	-	-
H0119R	0.580	2157.	1.250	-	-
H024R	0.613	2449.	1.500	$\pm$	-
H0121R	0.580	3019.	1.750	- to $\pm$	-
H027L	0.613	3265.	1.990	- to $\pm$	-

TABLE II EXPOSURE DATA cont.

Animal Number	Irradiance $Wcm^{-2}x10^{-3}$	Exposure Duration(s)	Radiant Exposure Jcm^{-2}	Classification Cornea / Lens	
		5-nm Bandwidth Exposures (cont'd)			
H0120R	0.580	3882.	2.250	H_C	-
H0133L	0.613	4081.	2.500	+	-
H023L	0.613	4082.	2.500	+	-
H0132L	0.613	4489.	2.750	++	-
H031L	0.709	5642.	4.000	+++	±
H042R	0.706	6374.	4.500	+++	H_L
H029R	0.688	7267.	4.990	+++	+
H041R	0.706	7790.	5.500	+++	+
H035R	0.688	8721.	6.000	+++	+
H074L	0.641	10924.	7.000	++++	+
		Waveband 320 nm			
		5-nm Bandwidth Exposures			
H078L	0.216	14000.	3.02	-	-
H067L	0.193	20725.	3.99	-	-
H0130R	0.302	23217.	7.00	- to ±	-
H0198R	0.369	20506.	7.50	*H_C	-
H0204R	0.437	17726.	7.75	± to +	-
H0193L	0.369	21660.	8.00	+	-
H081R	0.222	36036.	8.00	+	-

TABLE II EXPOSURE DATA cont.

Animal Number	Irradiance $Wcm^{-2}x10^{-3}$	Exposure Duration(s)	Radiant Exposure Jcm^{-2}	Classification Cornea / Lens	
		10-nm Bandwidth Exposures			
H0219L	1.02	1164.	1.19	-	-
H0221R	1.02	2910.	2.96	-	-
H0257R	1.63	3994.	6.50	-	-
H0265L	1.94	3497.	6.80	- to t	-
H0254L	1.63	4299.	7.00	*H_C	-
H0240R	1.27	5896.	7.50	+	-
H0238R	0.69	11439.	7.99	+	-
H0253R	1.45	6174.	9.00	+ to++	-
H0241R	1.27	7860.	10.00	++	-
H0265R	1.94	5142.	10.00	++	-
H0277R	1.64	7317.	12.00	++	- to $\pm$
H0291L	2.65	4749.	12.60	++	H_L
H0281L	1.42	9331.	13.30	+++	+
H0269L	1.63	9513.	15.50	+++	+

*λ320 H_C was taken as the mean of the 5 nm and 10 nm threshold exposures or 7.25 J/cm^2.

		Waveband 325 nm			
		10-nm Bandwidth Exposures			
H0267R	1.180	12712.	15.0	-	-

TABLE II EXPOSURE DATA cont.

Animal Number	Irradiance $Wcm^{-2}x10^{-3}$	Exposure Duration(s)	Radiant Exposure Jcm^{-2}	Classification Cornea / Lens	
		10-nm Bandwidth Exposures (cont'd)			
H0282L	1.756	10251.	18.0	H_C	-
H0271R	1.200	16667.	20.0	+	-
H0284R	1.756	14237.	25.0	+	-
H0299R	1.443	24440.	35.3	++	-
H0289R	1.727	23162.	40.0	++	-
H0309L	1.405	36000.	50.58	+++	-
		Waveband 335 nm			
		5-nm Bandwidth Exposures			
H011L	0.358	10800.	3.86	-	-
H047R	0.601	9983.	6.00	-	-
H052R	0.613	14683.	9.00	-	-
H056R	0.639	16435.	10.50	-	-
H069R	0.592	18581.	10.99	-	-
H054L	0.597	20100.	12.00	-	-
H087R	0.571	26290.	15.00	-	-
		10-nm Bandwidth Exposures			
H0243R	2.33	6450.	15.00	-	-
H0264R	1.84	10800.	19.90	-	-
H0261R	1.84	13680.	25.20	- to $\pm$	-

TABLE II EXPOSURE DATA cont.

Animal Number	Irradiance $Wcm^{-2}x10^{-3}$	Exposure Duration(s)	Radiant Exposure Jcm^{-2}	Classification Cornea / Lens	
		10-nm Bandwidth Exposures (cont'd)			
H0270L	1.89	14558.	27.50	±	-
H0244L	2.33	12888.	30.00	H_C	-
H0272L	1.93	20714.	40.00	+	-
H0292L	2.22	22502.	50.00	++	-
H0308L	2.28	26339.	60.00	++	-
		Waveband 345 nm			
		10-nm Bandwidth Exposures			
H0314R	0.964	51872	50.00	±	-
		Waveband 355 nm			
		10-nm Bandwidth Exposures			
H0282R	2.560	17578.	45.0	±	-
H0300R	2.630	18258.	48.0	±	-
H0273R	2.580	19380.	50.0	H_C ± to +	-
H0294R	2.560	27368.	70.0	+ to ++	-
		Waveband 365 nm			
		5-nm Bandwidth Exposures			
H073L	1.170	17094.	20.0	-	-
H075R	1.136	22007.	25.0	-	-

TABLE II EXPOSURE DATA cont.

Animal Number	Irradiance $Wcm^{-2}x10^{-3}$	Exposure Duration(s)	Radiant Exposure Jcm^{-2}	Classification Cornea / Lens	
		5-nm Bandwidth Exposures (cont'd)			
H0153R	1.087	27600.	30.0	-	-
H0171L	1.247	62239.	42.5	- to ±	-
H0170L	1.129	37641.	42.5	- to ±	-
H0166L	1.156	38914.	45.0	±	-
H0163R	1.375	36377.	50.0	±	-
H0167R	1.285	47000.	60.4	+	-
H0171L	1.125	62239.	70.0	+	-
		10-nm Bandwidth Exposures			
H0281R	5.560	8993.	50.0	±	-
H0285R	6.870	8006.	55.0	-	-
H0324L	4.734	12673.	60.0	-	-
H0326R	5.127	12678.	65.0	H_C	-
H0246R	7.091	14400.	102.0	+	-
H0288L	6.870	17470.	120.0	+	-
H0315R	5.629	28800.	162.0	+++	-
		Waveband 375 nm			
		10-nm Bandwidth Exposures			
H0320R	2.041	30000.	58.8	-	-

TABLE II EXPOSURE DATA cont.

Animal Number	Irradiance $Wcm^{-2}x10^{-3}$	Exposure Duration(s)	Radiant Exposure Jcm^{-2}	Classification Cornea / Lens	
		Waveband 385 nm			
		10-nm Bandwidth Exposures			
H0322R	0.979	30000.	28.2	-	-
		Waveband 395 nm			
		10-nm Bandwidth Exposures			
H0327L	0.816	30000.	23.5	-	-
		PRIMATE EXPOSURES			
		Waveband 300 nm			
		5-nm Bandwidth Exposures			
H0BB1L	0.627	15.9	0.01	$H_C \pm$	-
H0BB2R	0.627	31.9	0.02	+	-
H0BB4R	0.627	63.8	0.04	+	-
H0BB3L	0.627	127.7	0.08	++	-
H0BB3R	0.627	159.6	0.10	+++	-
H0BB5L	0.627	191.5	0.12	+++	- to $\pm$ H_L
H0BB4L	0.627	255.3	0.16	+++	$\pm$
H0BB1R	0.627	319.2	0.20	++++	+ ?*
H0BB2L	0.627	478.8	0.30	++++	+ ?*

* Could not study the lens adequately because of the severity of corneal damage.

The corneal threshold H_C of 0.012 Jcm^{-2} at 290 nm was taken from a previous study.[54,55] Exposures were not originally planned for wavelengths below 300 nm but the lower wavelength of the spectrum for lenticular opacities needed to be established. The radiant exposure of 3.0 Jcm^{-2} resulted in an opaque cornea which made it difficult to evaluate the lens. The cornea showed severe damage throughout all layers including the endothelium. A rather severe anterior uveitis involving the iris was evident (Figure 14) at 48 hours after exposure, the anterior uveitis had recovered spontaneously, the epithelial layers of the cornea had cleared but stromal haze and stromal opacities were evident. The damage was so severe that it was impractical to continue with higher radiant exposures at 290 nm. The cornea should act as a protective barrier for ultraviolet radiation at 290 nm and below.

At 295 nm, the radiant exposure required to produce a positive lenticular disturbance (Figure 15) also produced an immediate corneal reaction with epithelial haze, granule formation, stippling, and anterior stromal haze over the entire irradiated area. The epithelium stained extensively with sodium fluorescein confirming the immediate response. The severity of the reaction increased to complete exfoliation of the irradiated area at 20 hours post-exposure. The anterior stromal haze of the cornea also increased as the radiant exposure increased. The anterior chamber, iris, and lens were difficult to see with radiant exposures exceeding 0.75 $Jcm.^{-2}$ Severe anterior uveitis was seen at one hour post-exposure with a radiant exposure of 0.75 $Jcm.^{-2}$ Recovery was complete within 24 hours after exposure.

Radiant exposures above 0.3 Jcm^{-2} at 300 nm (2 x H_L) resulted in immediate corneal damage. The animal displayed extreme photophobia. Permanent damage resulted to the corneal epithelium, stroma, and endothelium. There was a thickening of the cornea and a dense posterior stromal striate. The iris was swollen with a sluggish pupillary response. The anterior chamber demonstrated a slight flare and a few cells were found in the aqueous. The corneal thickening indicated an interference with the normal metabolism of the endothelium. Minor anterior uveal changes were found at a 0.2 Jcm^{-2} radiant exposure which returned to normal within three days. Below 0.2 $Jcm,^{-2}$ anterior uveal changes were not found.

At 305 nm, radiant exposures above 0.3 Jcm^{-2} resulted in granules, opacities, stippling and fluorescein staining of the corneal epithelium. In addition, the stroma of the cornea was hazy and developed opaque striae after about 8 days. Within 24 hours, there were severe fibrinous endothelial deposits. An aqueous flare was noted within 4 hours post-exposure but was reduced in severity within 24 hours. All signs of anterior uveal inflammation disappeared within 8 days. There was an exfoliation of iritic tissue within 24 hours after exposure at the 1.0 Jcm^{-2} radiant exposure. Below 0.3 $Jcm,^{-2}$ no anterior uveal changes were found at 300 nm. There was a general increase in corneal damage as the radiant exposure was increased above the corneal radiant threshold of 0.04 $Jcm.^{-2}$ The radiant exposures at 310 nm followed the same pattern as observed at 305 nm.

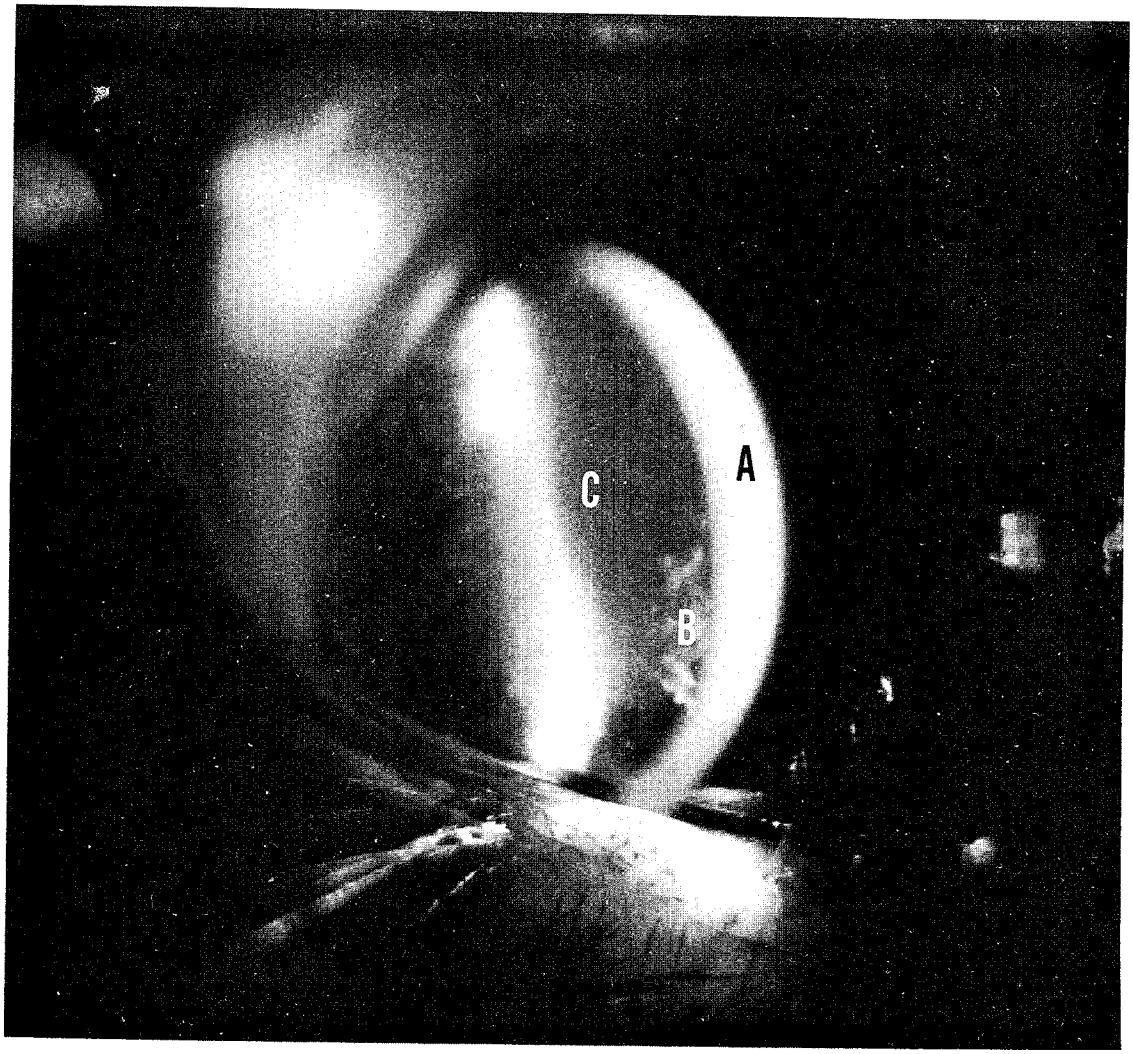

Figure 14: An optical section of the anterior segment of the eye which demonstrates anterior uveitis: cornea, A; membraneous inflammatory by-products on the corneal endothelium, B; and aqueous flare, C. Animal HO8OR, 305 nm, radiant exposure 0.5 J/cm^2, 27 hours post-exposure.

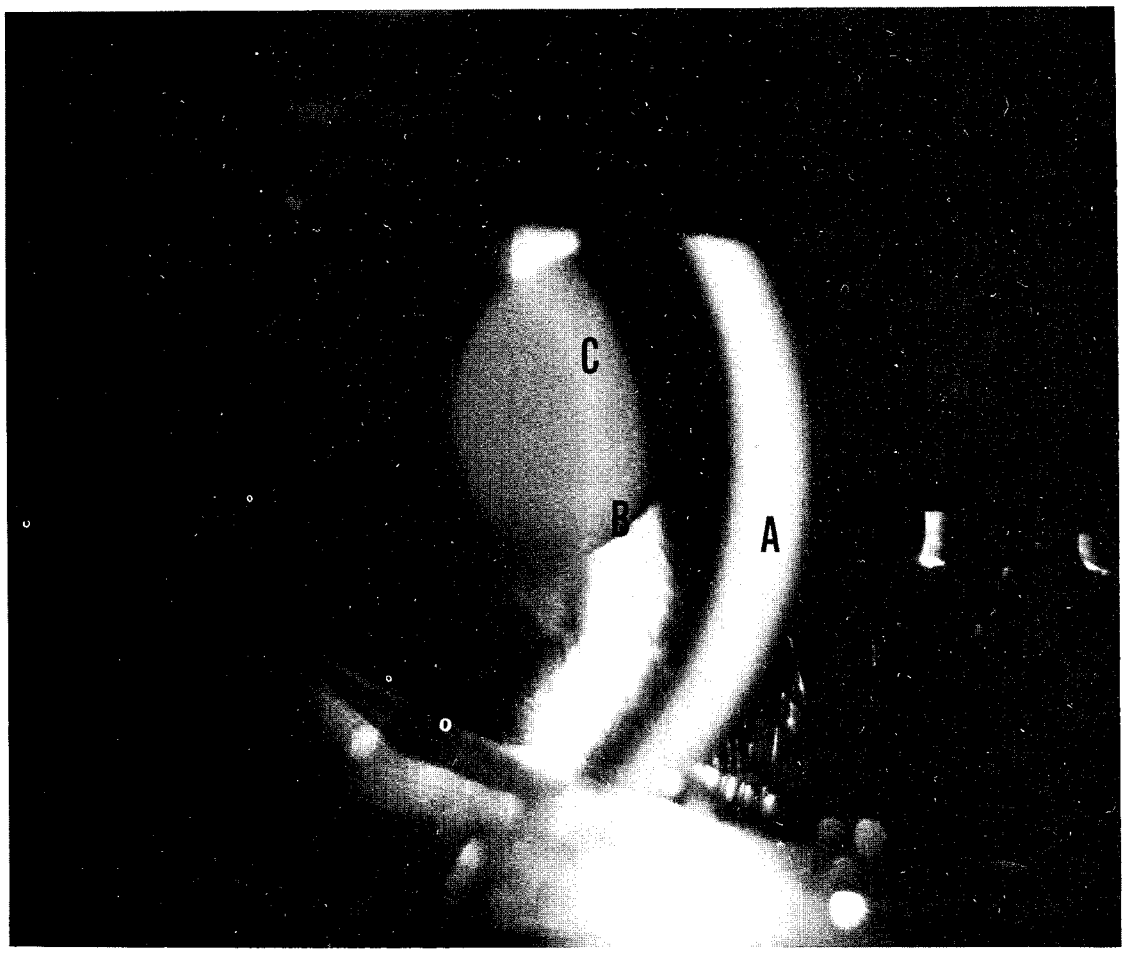

Figure 15: Ultraviolet lenticular damage. The optical section demonstrates the cornea; A; dot-like, discrete anterior subcapsular opacities, B; and the anterior suture line, C, a vertical whitish line bisecting the pupil. Animal HOCR, 310 nm, and 1.5 J/cm^2 radiant exposure, 24 hours post-exposure (2 x Q_L).

TABLE III ULTRAVIOLET THRESHOLD DATA FOR THE RABBIT CORNEA AND LENS

Wavelength in Nanometers	Corneal Radiant Exposure Threshold J/cm^2	Lens Radiant Exposure Threshold J/cm^2
290	0.012	>3.00
295	0.02	0.75
300	0.05	0.15
305	0.07	0.30
310	0.055	0.75
315	2.25	4.50
320	7.25	12.60
325	18.00	>50.00
335	30.00	>60.00
345	50.00	>50.00
355	50.00	>70.00
365	65.00	>162.00
375	>58.80	>58.80
385	>28.20	>28.20
395	>23.50	>23.50

At 315 nm, no anterior uveal or aqueous changes were found with radiant exposures up to 7.0 $Jcm.^{-2}$ The general pattern of epithelial granules, epithelial haze, and stromal haze increased in severity as the radiant exposure increased. Fluorescein showed a generalized, diffuse staining of the epithelium with no staining of the stroma. The response of the cornea and anterior uvea was not as dramatic at 315 nm in spite of the levels of radiant exposure being very high by comparison. At exposure levels above the lens threshold, there was increased involvement of the deeper corneal layers except for the endothelium. The lens showed an increased prominence of the anterior suture line, loss of the orange-peel appearance of the anterior capsule and small "salt-like" opacities throughout the anterior subcapsular epithelium. The lenticular opacities regressed to a concentrated area near the anterior suture line within 10 days and then migrated into the anterior cortex close to the anterior suture line by 21 days. These cataracts were considered permanent.

Radiant exposures at 320 nm showed a generalized involvement of the epithelium and stroma as the radiant exposures exceeded corneal threshold. There was an increase in stromal haze with stromal opacities being in isolated areas scattered throughout the exposed area. These signs became permanent as 10 Jcm^{-2} radiant exposure was given. The reaction of the lens to exposure was almost identical to that found at wavelength 315 nm. Permanent lenticular opacities were achieved at 15.5 Jcm^{-2}. The initial response showed "salt-like" opacities scattered throughout the exposed area of the lens. The scattered opacities migrated together, toward the anterior suture line, and formed two dense areas on both sides of the anterior suture line within 8 days. The cornea showed moderate stromal haze and stromal opacities. These ocular signs were considered permanent. Endothelial damage was not found at 320 nm.

The corneal response to the radiant exposures at 325 nm was almost identical to the corneal response found at 320 nm. As exposures were given above corneal threshold, the epithelium and stroma showed increased haze and scattered opacities. The corneal damage increased in severity as the radiant exposure increased. Permanent corneal damage was found at 40 Jcm^{-2} with the epithelium and the stroma being the corneal layers primarily involved. Lenticular damage was not found with radiant exposures as high as 50 Jcm^{-2}. These results indicate that the cornea acts as a protective barrier to the lens and that lens damage requires extremely high radiant exposures. The endothelial, integrity was not disturbed with exposures at 325 nm.

The radiant threshold for the cornea at 335 nm was 30 Jcm^{-2}. Lens threshold was not achieved with exposures up to 60 Jcm^{-2}. Above corneal threshold, increased radiant exposures resulted in epithelial debris, epithelial haze, epithelial granules, stromal haze and stromal opacities. The lens response was a slight increase in the prominence of the anterior suture line but the "orange-peel" appearance of the anterior capsule remained.

There was not a sufficient irradiance at 345 nm to make a thorough study of the cornea and the lens without exposures exceeding 14 hours. At 50 Jcm^{-2}, the cornea showed

some epithelial granules and epithelial haze. This exposure level was almost threshold for the cornea but additional exposures are needed to be able to rely on the data for threshold responses. This was not felt to be critical since the response which was obtained did not differ from the 335 nm and 355 nm responses.

At 355 nm, the corneal threshold was established at 50 Jcm^{-2}. Immediately after exposure, the cornea showed positive epithelial granules, epithelial haze, stromal haze and stromal opacities. All signs disappeared within 48 hours except for a residual stromal haze. An 8 hour (28,800 S.) 70 Jcm^{-2} exposure with an irradiance of 2.56×10^{-3} Wcm^{-2} resulted positive corneal epithelial granules, epithelial haze, stromal haze, increased prominence of the lens anterior suture line and a loss of the lens capsule "orange-peel" appearance. The lens disturbance returned to normal within 24 hours but the corneal damage persisted. No lenticular opacities were seen.

The corneal threshold radiant exposure at 365 nm was 65 Jcm^{-2}. Radiant exposures above the corneal threshold resulted in minimal additional corneal damage until about 100 Jcm^{-2} was achieved. Above 100 Jcm^{-2}, the stroma showed increase haze and isolated opacities which were usually evident through 48 hours. There was a dramatic increase in corneal damage with the 162 Jcm^{-2} radiant exposure. The epithelial granules were deep and coalesced centrally into a rather dense whitish haze. The stroma showed haze, opacities, and an increase in thickness. An area of the endothelium was krinkled in appearance with the border of the area showing "curled edges" of the endothelium. The corneal thickness had increased about 200% but was isolated to the area of endothelial damage. All of these ocular signs were seen immediately after exposure and were present for 48 hours when the eye was enucliated for histological study. The lens anterior suture line became more prominent and the orange-peel appearance of the anterior capsule disappeared; however, no lenticular opacities were seen. These results indicate that ocular damage does occur at high radiant exposure levels at almost any portion of the UV spectrum.

The levels of radiant exposure were not sufficient to establish a threshold response for the cornea or the lens at wavelengths 375 nm, 385 nm and 395 nm. The exposure durations were 8 hours (28,800 S.) but the spectral irradiance was too low to cause ocular effects. It is suspected that very high radiant exposures are required in this area of ultraviolet since ocular transmission increases above 370 nm. Further, the levels of exposure achieved may have resulted in retinal damage.

At the ultrastructural level, the discreetness of the ultraviolet-induced damage becomes apparent with individual affected cells located among healthy cells. Figure 16 shows that some cells retain a normal cytology even though they have been irradiated with twice threshold exposures of ultraviolet radiation. The surface corneal epithelial cells retain their squamous morphology with normal microvilli and attachments to deeper cells. The nuclei are flattened, parallel to the corneal surface, and have normal chromatic distribution. Other observable organelles appear to have a normal morphology. Although surfaced cells are sloughing off (Figure 17), the necrotic appearance of these cells mimics that observed in the normal cornea; i.e., the cells have

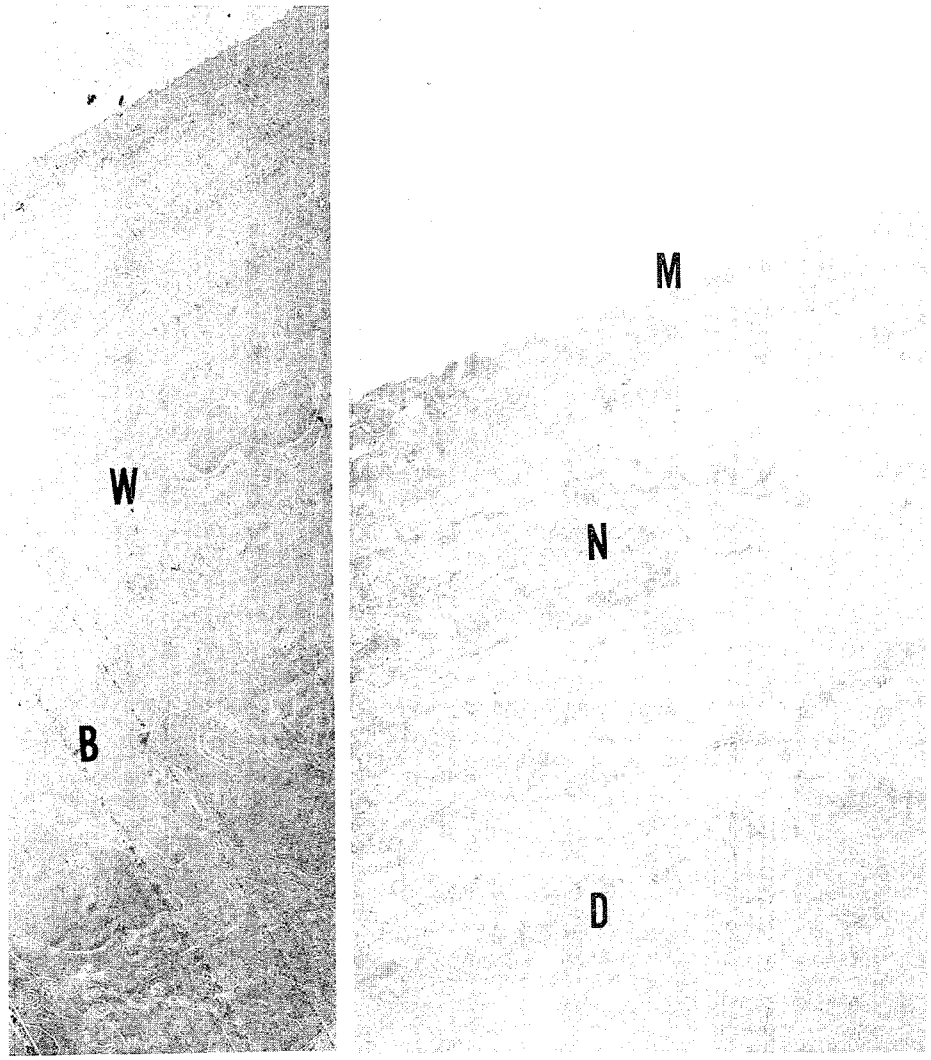

Figure 16a: Section through the corneal epithelium exposed at 305 nm with 0.15 Jcm^{-2} and prepared for electron microscopy 24 hours after exposure. Note normal appearance of the tissue (W - wing cells; B - basal cells) (2600 X).

b: Section through the surface epithelial cells of the same cornea. Note normal appearance of microvilli (M), cell borders, nucleus (N) and desmosomes (D) (13,200 X).

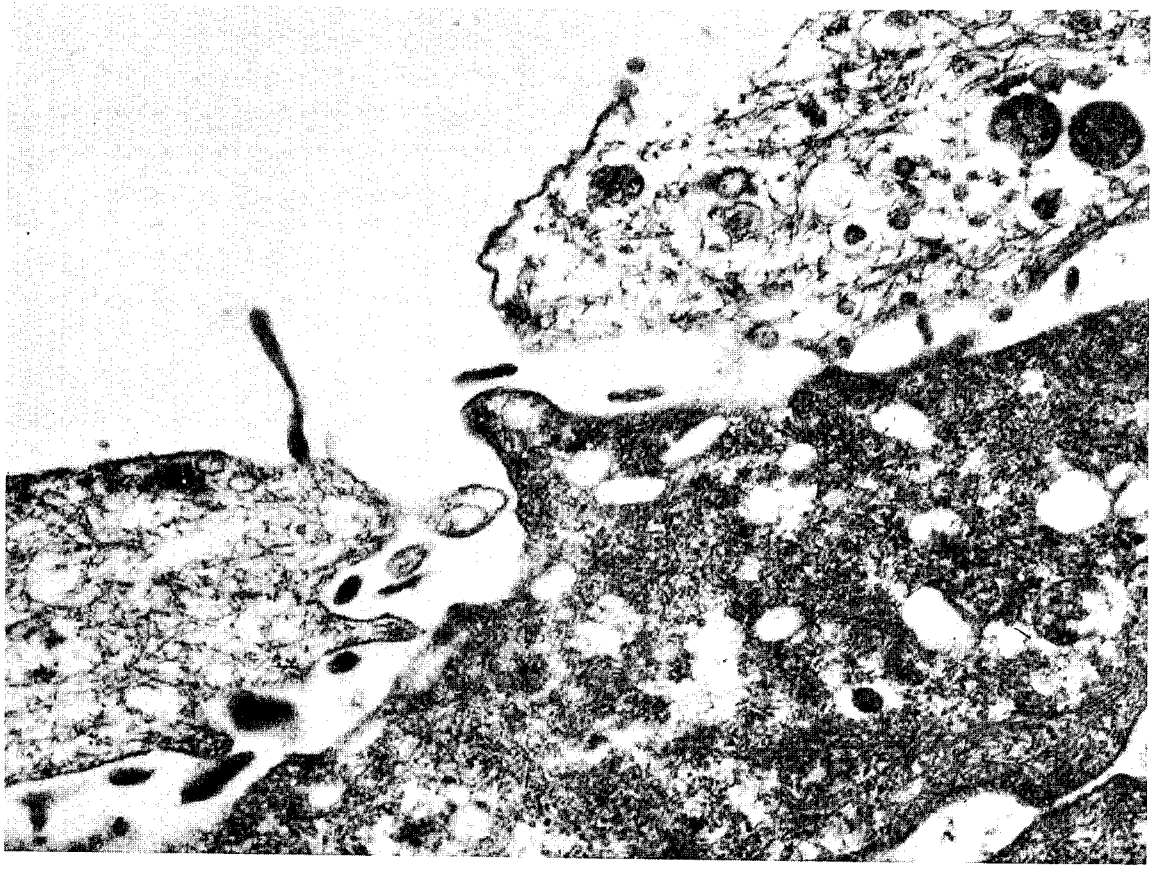

Figure 17: Desquamation of superficial cells 4 hours following exposure to 0.04 Jcm^{-2} at 295 nm. The absence of microvilli, breakdown of cell membranes, vacuolation, and other necrotic activity within the cells are evident in both the superficial and the intermediate underlying cells[61] (49,000 X).

lysosomal activity, the lysosomes are small, and the lysosomes are relatively few in number. It is probable that in the early hours following ultraviolet exposure there may be an acceleration of desquamation which accounts for the clinical and cytological observations. Eight hours after exposure to twice the corneal threshold, the lysosomal activity is seen to have increased dramatically both in extent and magnitude (Figure 18). The material within the lysosomes is relatively homogeneous and electron dense. The other organelles of these outer cells are in an early state of degeneration (Figure 19).

The wing (intermediate) cells vary from normal to grossly necrotic. Figure 16 shows a cornea exposed at twice corneal threshold. The cells do not differ substantially from normal cells. There is no disturbance of the nucleus or other organelles and the cell membranes and desmosomes are intact. The cells have maintained their polyhedral configuration. Many nuclei have assumed a position parallel to the surface of the epithelium. However, they do not have the flattened appearance of the surface cells. Normal chromatic distribution is maintained. The entire intermediate and basal layer of cells also show deeper staining. In contrast, Figure 19 demonstrates the severe cellular damage to the wing cells by similar irradiance levels. What appears to be giant lysosomes have light structures in varying stages of degradation. These organelles are in close proximity to the nucleus. It is possible to see agregations of lysosomes displaying their macrophagic activity. This "autophagocytosis" increases to engulf the entire cell as seen in Figure 20. It is possible that these cytological changes are the basis for the biomicroscopically observed "granules". Further evidence is currently being analyzed. With these levels of radiant exposure, the basal cells observed were normal. Similarly, the stroma, Descemet's membrane, and the endothelium exhibited no variation from normal.

During the final month of the research, nine primate (Galago senegalensis) eyes were exposed to selected levels of ultraviolet radiation at 300 nm with 5.0 nm full-bandpass (Table II). Corneal involvement followed a similar pattern to the rabbit with a delayed threshold at 0.01 Jcm^{-2} and an immediate response at 0.3 Jcm^{-2} (Table 2). The animals were not retained for sufficient length of time to establish permanent damage. Lens disturbance consisting of an increased prominence of the anterior Y suture and a few granules located in anterior epithelium was found at 0.12 Jcm^{-2}. Unfortunately, it was not possible to examine the lens thoroughly at higher irradiances because of the severe corneal reaction. Thus, although the number of primate eyes were limited, the cornea appears to protect the lens from low irradiance, long term exposures much like the rabbit. In contrast with the rabbit, anterior uveitis was not found but occasional cells were observed in the aqueous of the anterior chamber, particularly at the radiant exposures above 0.10 Jcm^{-2}.

A summary of the effects of ultraviolet radiation on the eye may assist in an understanding of these complex interactions. Corneal changes followed a rather consistent pattern of involvement as the radiant exposure and wavelength increased. Above threshold, radiant exposures resulted in an increase in epithelial debris up to about 320 nm where epithelial debris remained relatively constant at longer

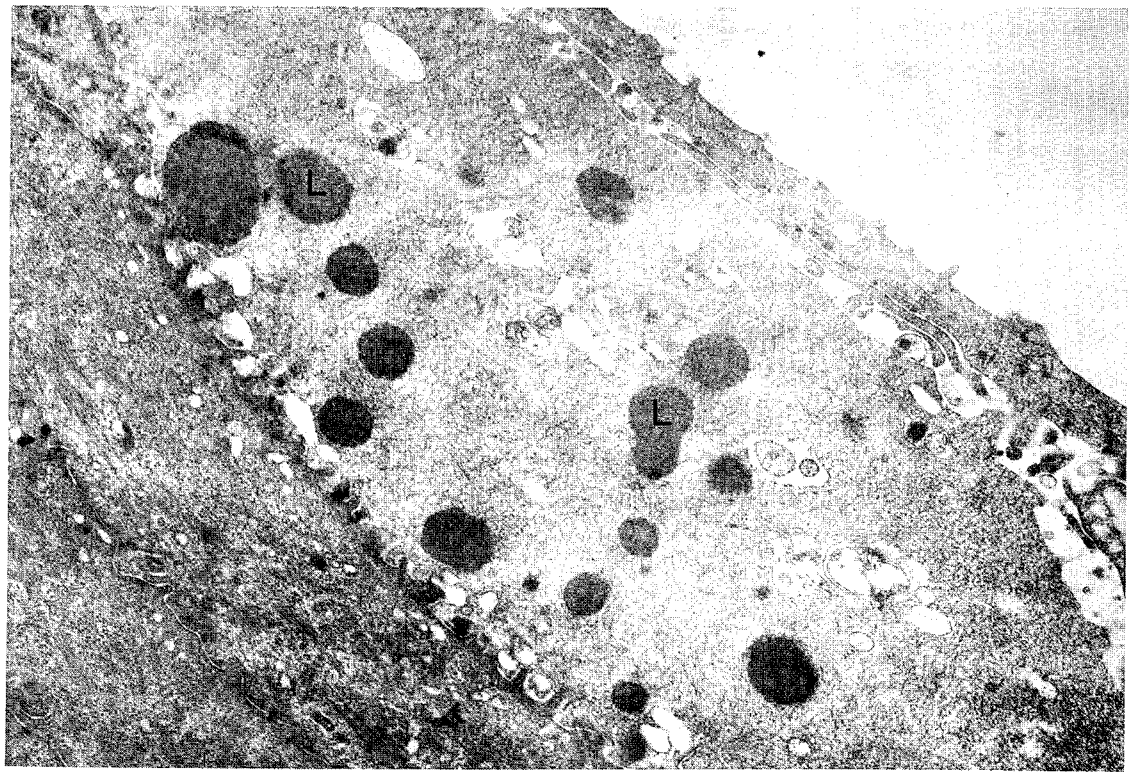

Figure 18: Lysosomal activity 8 hours after two irradiations with 0.02 Jcm^{-2} separated by 8 hours at 295 nm. The lysosomes (L) appear relatively homogeneous and electron dense. This activity is occuring early in the vacuolation stage of cellular degeneration[61] (12,000 X).

Figure 19: Severe damage to a wing (intermediate) cell produced by 0.04 Jcm^{-2} at 295 nm 12 hours following irradiation. There are less electron dense areas within a giant lysosome (L). Other evidence of degeneration of the cell is apparent [61] (9,000 X).

Figure 20: A wing (intermediate) cell of the corneal epithelium 18 hours after a radiant exposure of 0.05 Jcm^{-2} at 295 nm. The lysosomal activity L now engulfs almost all of the entire cell except for the nucleus[61] N (9,700 X).

wavelengths. The epithelial granules increased in number, then coalesced to form a syncytiun or network which increased in density following higher radiant exposures. Epithelial damage, epithelial stippling and epithelial haze increased in severity as the radiant exposure was increased. In contrast, corneal damage appeared to shift from the external epithelial corneal layers to the internal stroma as wavelength increased above about 315 nm. At the same time, stromal granules, stromal haze and stromal opacities increased with increased radiant exposures. There appeared to be two reactions present in wavelength above about 320 nm with high exposure levels. Immediately after exposure, the epithelial layers of the cornea showed a moderate response with a minimal response from the stroma. The epithelial layers showed minimal responses with an increasing stromal effect at 24 hours after exposure. Both the epithelium and stroma showed severe reactions when extremely high exposures were given regardless of the wavelength. Thus, there appears to be both a wavelength and a radiant exposure response with the depths of the cornea becoming more involved at longer wavelengths and at higher exposure levels. Endothelial changes were found usually within 4.5 hours after exposure at wavebands below 315 nm of approximately 2 x H_C resulted in irreversible damage to the cornea.

High corneal exposures below the 315 nm waveband were accompanied by secondary anterior uveitis. Anterior uveitis is characterized by ciliary injection, aqueous flare, and membranous inflammatory by-products deposited on the corneal endothelium. (Figure 14). Anterior uveitis made it difficult to observe the lens or its capsule. Anterior uveitis usually regressed spontaneously within approximately two days. Table IV provides information on the wavelength, radiant exposure, time after exposure and time to recover from anterior uveitis. It is apparent from Table IV than anterior uveitis was not induced by ultraviolet radiant exposures above 315 nm.

A description of UV induced lenticular damage was not available in the literature from which lenticular damage criteria could be compared. The first biomicroscopic signs of lenticular damage were (1) loss or reduction of "orange-peel" appearance of the anterior capsule and (2) an increased prominance of the anterior suture line. These two biomicroscopic signs usually regressed to normal within 24 hours post-exposure. As the radiant exposure approached threshold, many small, discrete white dots appeared in the anterior sub-capsular epithelium of the lens (Figure 15). These anterior sub-capsular opacities had a similar appearance to the corneal epithelial granules. Table V presents the wavelength, the radiant exposure necessary to produce the lenticular opacities, the time of appearance of the lenticular opacities after exposure, and the time of disappearance of the lenticular opacities after exposure.

Supra-threshold exposures to the lens resulted in permanent lenticular opacities. The change from the small discrete white anterior sub-capsular dots into the permanent opacities developed in an orderly manner. The fine discrete opacities migrated posteriorly into the anterior cortex of the lens. Animals followed for extended periods of time after exposure did not show nuclear or posterior sub-capsular opacities. At the same time, an increase in the lens stromal haze was detected. The fine opacities organized into fewer, more dense opacities. The permanent opacities usually developed in proximity to the anterior suture line. In addition to the permanent opacities,

TABLE IV ANTERIOR UVEITIS

Wavelength	Radiant Exposure Jcm^{-2}	Time After Exposure	Recovery
295	0.75	1 hour	24 hours
300	0.50	24 hours	48 hours
305	0.30	24 hours	48 hours
310	1.00	2 hours	24 hours
315	No anterior uveitis found at the highest exposure level		
320	No anterior uveitis found at the highest exposure level		
335	No anterior uveitis found at the highest exposure level		
345	No anterior uveitis found at the highest exposure level		
355	No anterior uveitis found at the highest exposure level		
365	No anterior uveitis found at the highest exposure level		
375	No anterior uveitis found at the highest exposure level		
385	No anterior uveitis found at the highest exposure level		
395	No anterior uveitis found at the highest exposure level		

TABLE V TRANSIENT LENTICULAR OPACITIES

Wavelength nm	Radiant Exposure Jcm^{-2}	Appearance of Lens Opacities	Disappearance of Lens Opacities
295	0.75	2 hours	2 days
300	0.15	12 hours	3 days
305	0.30	24 hours	7 days
310	0.75	24 hours	2 weeks
315	4.50	48 hours	1 week
320	12.60	24 hours	3 days
325	50.00	Transient opacities not achieved	
335	60.00	Transient opacities not achieved	
345	50.00	Transient opacities not achieved	
355	70.00	Transient opacities not achieved	
365	162.00	Transient opacities not achieved	
375	58.80	Transient opacities not achieved	
385	28.20	Transient opacities not achieved	
395	23.50	Transient opacities not achieved	

occasionally vacuoles were present. Table VI presents the wavelength, radiant exposure, and the appearance of the permanent lenticular opacities following exposure and demonstrates that permanent lenticular opacities were not induced until the radiant exposure reached 2 x H_L.

The primate corneal involvement followed a similar pattern to that of the rabbit but showed a lower corneal threshold. The evaluation of the primate lens was difficult; however, those signs which could be observed were similar to the rabbit lens.

Ultrastructure investigations confirm the presence of discrete vesicles of a necrotic nature with moderate to severe cellular degeneration related to the time after exposure at equivalent radiant exposures for two wavelengths. The damage was particularly extensive in the intermediate and surface layers of the corneal epithelium.

TABLE VI PERMANENT LENTICULAR OPACITIES

Wavelength nm	Radiant Exposure Jcm^{-2}	Appearance of Lens Opacities
295	1.0	60 hours
300	0.5	24 hours
305	0.5	24 hours
310	1.5	24 hours
315	6.0	24 hours
320	15.5	24 hours
325	50.0	Permanent opacities not achieved
335	60.0	Permanent opacities not achieved
345	50.0	Permanent opacities not achieved
355	70.0	Permanent opacities not achieved
365	162.0	Permanent opacities not achieved
375	58.8	Permanent opacities not achieved
385	28.2	Permanent opacities not achieved
395	23.5	Permanent opacities not achieved

DISCUSSION

Figure 12 illustrates the corneal and lenticular threshold data. The upper limit for the action spectrum for the cornea extends to about 320 nm because the radiant exposure of 7.5 Jcm^{-2} is a factor of 1.5×10^3 greater than the corneal threshold of 0.005 Jcm^{-2} at 270 nm. The action spectrum for UV induced lenticular cataracts begins at 295 nm and extends to 320 nm. Corneal damage at 290 nm with 3.0 Jcm^{-2} and at 325 nm with greater than 50 Jcm^{-2} was so severe that the reduced transmittance of the cornea prevented the exposure to the lens from inducing cataracts. Thus, the wavelengths which induce UV cataracts are only 25 nm in waveband width and, at the same time, are extremely efficient in producing ocular damage. The ocular damage resulting from exposure to the 295 nm - 320 nm waveband includes the epithelium, stroma, endothelium, iris and lens. The threshold radiant exposures from non-coherent sources for corneal damage are sufficiently below the radiant exposure levels required to produce lens damage that the cornea should serve as a protective barrier for the lens. However, in the 295 nm to 320 nm wavelength range, corneal damage is not severe enough to prevent lenticular damage if the incident irradiance were sufficiently high and given in a relatively short duration; therefore, even though the cornea should act as a protective barrier, lenticular damage may be induced.

The concept of an action spectrum does not intend to convey or infer that wavelengths outside the action spectrum cannot produce ocular damage. The action spectrum concept does indicate that the efficiency of ultraviolet radiation in producing ocular damage is quite high and that extraordinary conditions must be encountered to produce ocular damage from wavelengths outside the action spectrum. In fact, corneal damage was induced at 325 nm and above but the radiant exposure levels are quite high. Thus, under normal environmental conditions, it would be extremely remote that wavelengths outside the action spectrum would produce ocular damage because the radiant exposure levels required to produce ocular damage are extremely high when compared to the threshold values.

The question relative to the validity of the threshold data needs to be addressed so that one may judge the confidence which may be placed in the data. There are different parameters of the experimental procedures which may contribute to the uncertainty of the results. These include the precision with which the source can be measured, stability of the source output, the ability to align the animal's cornea normal to the optical beam, eye movements which occur during the exposure, the ages of the different animals, the ability of the researchers to use the criteria and classify the effects of the exposure, and exposure duration were all sources of error. Each of these topics will be discussed in the context of the experimental protocol.

The NBS has recently published a bulletin on the uncertainties and limitations in UV spectroradiometry.[60] The bulletin concludes that a typical state-of-the-art laboratory measurement uncertainty is about 6%. The EG&G measurement system used in this

study was NBS standardized. Further, it was cross-calibrated against the NBS standard 1000 W tungsten filament, quartz-halogen lamp, and an NBS standardized Eppley thermopile. The NBS standard deuterium UV source became available in January 1977 and the system is being assembled for further cross-calibration study. Measurements could be repeated on a daily basis at a selected wavelength within approximately 2% accuracy. It was estimated that when all factors of uncertainty were considered, the measurement error was approximately $\pm$10%.

The stability of the source output is determined partially by the power supply. The power supply was regulated to $\pm$0.5% which should have reduced power fluctuations to a minimum. Repeated measurements of the wavelength used for exposure before and after an experimental session revealed a less than 10% irradiance fluctuation. Adequate and constant cooling of the arc lamp assisted in maintaining a constant source output because the output of arc lamps varies with the temperature of the lamp. Thus, it was considered that the stability of the source was adequate to assure reliable data.

The alignment of the eye in the optical beam was a relatively simple task and could be repeated precisely from animal to animal. To align the eye, the monochromator was set at 450 nm. The optical beam illuminated the cornea and the pupil with a bright reflex was seen at the apex of the cornea. The corneal reflex was aligned in the center of the pupil and this position was maintained throughout the duration of the exposure. The distance from the cornea to the exit slit of the monochromator was measured using the corneal reflex. During exposure, the cornea and lens of the eye provided a fluorescence which allowed the investigators to maintain alignment of the eye.

A special holder was designed to restrain the animal during exposure and to allow the examination of the eye with the biomicroscope. However, it is impossible to design a constraint system which will prevent all body, head, and eye movements. Minimal head and eye movements were a problem which contributed to the variability of the data. The optical beam from the monochromator was large enough to insure that the animal's eye, especially the center of the cornea, would be in the optical beam in spite of eye movements. However, eye movements would result in a decrease in the radiant exposure because UV obeys the cosine law.[8] To minimize these effects, the optical beam was essentially collimated at the plane of the exposure. If the animal moved while being exposed, prompt realignment of the eye in the optical beam was accomplished. Therefore, the size of the optical beam and the fact that the optical beam was collimated assisted in reducing these uncertainties to a minimum.

The duration of the exposure increased the variability of the data. Short exposure durations were made without eye movements, data could be obtained from a large group of animals for each wavelength, and closer intervals between radiant exposure levels could be given. Each of these factors contribute to increased confidence in the threshold response. Long duration exposures resulted in an increase in eye movements, exposure of a smaller number of animals at each wavelength, and a larger interval between radiant exposure levels. However, one is reminded that the ability to measure the source was $\pm$10% regardless of the level of radiant exposure and may have served to minimize these errors.

Each of the investigators were thoroughly trained in the use of the biomicroscope. Preliminary exposures were made in order to standardize the biomicroscopic procedure and the interpretation of the ocular damage. Two investigators independently evaluated the exposure damage and assigned criteria values to each structure examined. There were differences in the assigned criteria values between investigators of not more than one structure for each eye and, almost all the time, the criteria values were the same for a given evaluation. In most instances, neither investigator knew the exposure wavelength nor radiant exposure level prior to the evaluation of the eye. The classification of the ocular damage was made in consultation between the investigators. It was felt that the use of these procedures kept investigator variability and error to a minimum.

All animals used in the study were procured from the same husbandry and were from 2 to 2.5 kg in body weight. All exposures were made without anesthesia, analgesia, or tranquilizers to insure that drug effects would be minimized. It was felt that these precautions provided a uniform state in the animals throughout the period of the research.

It is important that confidence can be placed in the radiant exposure thresholds. First, threshold radiant exposures were made at the same wavelength over a period of three years at various intervals of time using the standard research procedures and the results were within 10%. Next, radiant exposure thresholds were established independently by different investigators at the same wavelength and it was found that the investigators could differentiate 10% increases or decreases in radiant exposures at threshold. These examples illustrate that investigator error was at least as small as the ability to measure the irradiance of the source and that the uncertainties listed above appear to average out over a period of time and between different investigators. Finally, it must be recognized that the data for wavelengths below 325 nm are more valid if, for no other reason, a greater number of animals were exposed at these wavelengths. The duration of the exposures required to attain the necessary radiant exposure levels above 325 nm must be considered when the validity of the data is discussed. In general, it is felt that the data below 325 nm are valid to within +10% or the ability to measure the source output accurately while the data above 325 nm are probably valid to within +15%. It is felt that these are acceptable figures when one considers that ocular damage which may result from an exposure in an industrial situation would be much more serious for exposures containing ultraviolet radiation at 325 nm and below.

On studying the data it becomes apparent that the radiant exposure levels necessary to produce ocular damage increases dramatically above 325 nm. The answer to this perplexing problem probably lies in the transmittance of the ocular media, the mechanism which causes the damage, the relative effectiveness of the particular wavelengths to produce ocular damage, the fluorescence of the ocular media, and possibly the combination of all of these inter-related phenomena. Each of these parameters will be discussed in order to attempt to answer the question.

It is well known that, in order for radiant energy to produce an effect, the radiant energy must be absorbed by the tissue in question. Transmittance data for the rabbit

eye which presently exists in the literature demonstrates that the UV wavelengths from about 300 nm to 370 nm are readily transmitted by the cornea and absorbed by the crystalline lens. It is these wavelengths which should be the most effective in producing UV lenticular cataracts. The data of this study clearly illustrate that the wavelength range from 295 nm to 320 nm are the most efficient in producing lenticular damage. Why, then, are the more readily transmitted wavelengths above 320 nm not as effective in producing lenticular damage? Is it that the longer UV wavelengths possess less quanta? If so, this problem could be overcome by extended exposure durations but the exposure durations required to induce lenticular and corneal damage far exceeds that necessary to equate wavelength quanta differences. The fact that the present transmittance data does not support producing lenticular opacities at 295 nm indicates that the transmittance data may be in error. Transmittance data were generated with instrumentation not designed for the UV spectrum; therefore, experiments on the transmittance of the ocular media in the UV spectrum need to be repeated and the data updated.

It is probable that fluorescence of the ocular tissue plays a major role in the efficiency of different wavelengths to produce corneal and lenticular damage. We have not been able to locate quantitive data on the spectral fluorescence of the ocular tissues. A qualitative experiment was made by visual observation while scanning the monochromator from 200 nm to 400 nm in 5 nm steps under the normal experimental conditions. There is a faint suspicion of corneal fluorescence below 270 nm which increases dramatically at 275 nm and continues to be predominant to 300 nm. Lenticular fluorescence is not discernable in the 275 nm to 300 nm wavelength range. From 300 nm to 310 nm, the corneal fluorescence begins to fade and the lenticular fluorescence increases in intensity. Above 310 nm, only a faint corneal fluorescence can be discerned, but there is a continuous increase in lenticular fluorescence between 310 nm and 325 nm. It is suspected that a faint corneal fluorescence continues but the lenticular fluorescence is so predominant that the corneal component is difficult to see. Above 325 nm, the fluorescence appears to be almost entirely lenticular with maxima at 335 nm, 365 nm, and 370 nm which is replaced with a deeper blue corneal and lenticular glow above 390 nm. These maxima correspond to the increased relative spectral irradiance of the source. It is suspected that the lenticular fluorescence continues to increase in intensity until about 380 nm where the deep blue corneal and lenticular glow predominate.

It is curious that the description of the fluorescence of the cornea and the lens corresponds remarkably well with the radiant exposure increases required to produce ocular damage. Therefore, it is suggested that fluorescence studies would provide quantified data which when used to correct radiant exposure data would demonstrate that the increase in radiant exposure was because a substantial portion of the incident energy was expended in fluorescence and was not available to produce ocular damage. This hypothesis is supported because fluorescence arises by direct emission after UV absorption. Fluorescence spectroscopy provides a very sensitive technique to identify the nature of the compounds undergoing fluorescence and permits detecting changes at very early stages. Fluorescence spectroscopy research is needed to negate or support the above hypothesis and to establish changes which occur in compounds of the cornea and lens as the result of ultraviolet exposure.

A comparison of the monochromator threshold data from this study with the laser threshold data is provided in Table VII. It can be seen that the monochromator data greatly exceeds the laser data. It may be that a comparison is not valid because the characteristics of the source used in this study differs greatly from a laser source. Exposures were of long duration, low irradiance (10^{-3} Wcm^{-2}), incoherent, and of large diameter (1.6 cm x 1.8 cm). The laser beam is coherent, of high irradiance and has an extremely small diameter. The radiant exposure levels required to produce corneal and lenticular damage with the laser took minutes while the radiant exposure for the high-pressure arc system took up to hours. These significant differences may make the comparison of laser exposures and broad-band exposures questionable. The laser data indicate that researchers using UV wavelengths must use extreme caution. However, the average worker in an industrial environment would more likely be exposed to relatively low power, large diameter, incoherent UV sources.

Zuclich and Connolly postulated the corneal damage to be photochemical and the lenticular damage to be thermal from laser exposures. These damage differences were based on a reciprocity relationship (Ixt = k) for corneal damage and the lack of reciprocity for lenticular damage. The data of Zuclich and Connolly show that the argon laser (351.1 nm and 363.8 nm) lenticular threshold was 76 Jcm^{-2} for a 4 second exposure and was 19 $\pm$ 1.8 Jcm^{-2} for 1 second exposures for a corneal irradiance of 19 Wcm^{-2}.

Two factors which may account for these differences in responses could be fluorescence and wavelength efficiency. Figure 12 demonstrates the action spectrum for the production of corneal and lenticular damage. The increased radiant exposure required to produce ocular damage could be due to the relative effectiveness of longer UV wavelengths in producing a photochemical reaction rather than being thermal in nature. The previous discussion on fluorescence provides sufficient evidence to demonstrate its involvement in the irradiation process. However, the high power, short duration of the laser exposures may induce thermal damage.

It is assumed that both the corneal and lenticular damage found in this study are photochemical. This assumption is based on the fact that the corneal and lenticular damage produced similar granular appearance when studied with the biomicroscope. Additionally, corneal and lenticular damage were not obtained at threshold radiant exposure levels until after a rather long latency while thermal damage usually occurs immediately after the tissue has been exposed. It may be that the low power, continuous, long duration exposures provided a radiant exposure which affected the lens in both a photochemical and thermal response because thermal exposure might have produced the same granular effect as UV exposure.

Several statements can be made relative to the biochemical studies. Near UV in the 300 nm to 400 nm wavelengths from the sun or artificial lights is transmitted by the cornea and maximally absorbed by the crystalline lens. Most of the research has been in vitro and on the mouse and dogfish. The corneas of these animals most probably do not

TABLE VII COMPARISON OF MONOCHROMATOR RADIATION THRESHOLDS WITH LASER RADIATION THRESHOLDS

	Corneal Threshold	Lenticular Threshold
Pitts, Cullen and Hacker	18.0 Jcm^{-2}	>50.0 Jcm^{-2}
325 nm	Reversible Damage	
Ebbers and Sears		
He-Cd Laser	0.8 Jcm^{-2}	6.5 Jcm^{-2}
325 nm	Reversible Damage	Permanent Cataracts
MacKeen, Sears and Fine		
He-Cd Laser	--------	28.0 Jcm^{-2}
325 nm		Permanent Cataracts
Zuclich and Connolly		
CW Krypton-ion laser	60-70 Jcm^{-2}	(Retinal Lesions)
350.6 + 356.4 1:3		
Nitrogen Laser	10 Jcm^{-2}	1 Jcm^{-2}
337 nm		

possess the same transmittance characteristics as the rabbit or human cornea and, thus, could not afford the same protection against the near UV. However, studies on human cataractous lenses demonstrate that some of the biochemical changes found for certain cataracts may be equivalent to the animal studies. The human lens does absorb most of the near UV in the 320 nm to 370 nm bandwidth which may cause photooxidation of isolated lens proteins, induce pigmentation, and an increase in crosslinking but the radiant exposures above 320 nm need to be quite high to produce an effect. The questions of whether lens protein is directly photooxidized by near UV, mediated by sensitizers inherent in the lens, or if free amino acids are photooxidized and bound covalently to the proteins has not been conclusively demonstrated.

Biochemical research indicates that exposure of the eye to near-UV for sufficient periods of time with a low irradiance comparable to the irradiance level of sunlight may interfere with the synthesis of lens proteins, may catalyze insoluble lens protein, and may result in chromatic changes in the lens. While the basic mechanism remains to be found, the evidence clearly demonstrates that both in vitro and in vivo exposure to the near UV can produce cataractous changes in the crystalline lens.

There are some additional implications from these data which need to be mentioned. While it is quite possible that the mechanism(s) which produced the observed ocular damage are photochemical, it does not necessarily follow that the same biomolecules are involved in each instance. It has been well documented that the nucleic acids are susceptible to UV induced damage at 260 nm and that amino acids are affected at 280 nm. Thus, it may well be that the integrity of a certain "family" of biomolecules is affected at a given wavelength in a given tissue and that a different group of biomolecules is affected at other wavelengths in differing tissues while both may undergo a change to a granular appearance. Therefore, the biochemical results strongly suggest the necessity for investigations into the mechanisms responsible for the observed ocular damage in order to fully describe the means whereby UV radiation of a given wavelength affects a given tissue.

There are several important areas of research on UV-induced cataracts which should be pursued. The present effort did not consider the problems of repeated subthreshold exposures whether or not subthreshold exposures are cumulative, the duration over levels of irradiance or radiant exposure. Subthreshold exposures become an important question because more workers are exposed to subthreshold exposures than are exposed at higher levels of irradiance. The answers to these and other questions related to subthreshold exposures need to be pursued.

The electron microscopic data were derived from two wavelengths (295 nm and 300 nm) and at equivalent radiant exposures of two times threshold at these wavelengths. The data verify the vesicular nature of the damage to the outer and intermediate layers of the corneal epithelium. The data also demonstrate the need for further electron microscopic investigations relating the degree of damage to the levels of radiant exposure, wavelength of exposure, and the time after exposure.

The role of additivity or synergism with other portions of the electromagnetic spectrum needs elucidation. The exposures made during this study were relatively pure

wavebands and were accomplished in a dark room. It is well known that the effects of ultraviolet radiation on the skin are enhanced by the visible and near infrared simultaneously irradiating the skin. The question arises as to whether the visible or infrared radiation added to the UV would result in a change in the threshold. Most of the human exposure to ultraviolet radiation results from sunlight which contains the visible and infrared spectra. This combination may make the human more susceptible to UV-induced cataracts. The role of the remainder of the spectrum may be additive or synergistic and needs defining.

Cataracts are the second leading cause of blindness in the United States. Considerable research on in vitro systems have identified biochemical alterations of lens proteins but have not actually addressed the causative factors. The significance of this study is that an animal model has been demonstrated and radiation levels have been established from which cataracts can be produced that vary from transient to permanent cataracts. Measurement instrumentation allow the definition of the radiant exposure to within +10%. Research should be done which provides an insight into the nature of cataractous changes at the molecular level, the sub-cellular level, localize the opacity and describe the opacifications. The information gained should provide a definitive solution to the problem of the mechanism of UV-induced cataracts in particular and radiation-induced cataracts in general. The interpretations can then be applied to the study of the mechanism of other cataracts. UV induced cataracts have taken on a more important consideration in public health and protection because many new industrial operations utilize ultraviolet radiation in their processes. The recent publications related to the loss of the ozone layer from aerosols and aircraft pollutants indicate that increased UV will reach the earth's surface and that UV waveband corresponds to the UV which is most effective in producing cataracts. Photochemistry and biochemistry provide the techniques to investigate the molecular and sub-cellular levels while the electron microscope can localize the damage at the cellular and organelle levels.

Finally, laboratory data are often difficult to translate into meaningful solutions of practical problems. The concept of the relative efficiency of the action spectrum provides a convenient method for computing safe exposure durations and the allowable transmittance of optical protective devices. The data required to calculate safe exposure criteria include the spectral irradiance of the source, the spectral transmittance of any optical media before the eyes, and the relative efficiency of the ultraviolet action spectrum to produce ocular damage. The radiant exposure threshold data for the action spectrum which produces lenticular cataracts are shown in Table VIII. The relative efficiency of the action spectrum is calculated by selecting the most efficient wavelength which produces the damage (300 nm) and dividing all radiant exposure values of the action spectrum into this radiant exposure value (Table VIII).

The total irradiance for the waveband of interest may be calculated as follows:

$$E_{(295-320)} = \sum_{320}^{295} E_\lambda T_\lambda W_\lambda \Delta_\lambda \qquad (1)$$

Where:

$E_{(295-320)}$ = total irradiance for the wavelength range in Wcm^{-2}

E_λ = spectral irradiance of the source in Wcm^{-2}

T_λ = spectral transmittance of the optical media in decimal form

W_λ = relative efficiency of the action spectrum produce lenticular cataracts

Δ_λ = waveband interval of the spectrum

The safe exposure duration t is given by:

$$t = \frac{H_{L300}}{E_{(295-320)}} \qquad (2)$$

Where:

t = safe exposure duration in seconds

H_{L300} = radiant exposure threshold for cataracts at 300 nm or 0.15 Jcm^{-2}

$E_{(295-320)}$ = total irradiance for the wavelength range in Wcm^{-2}

If it is assumed that the total spectral transmittance can not exceed mean transmittance T for the action spectrum, the transmittance T of a protective optical media may be found as follows:

$$T = \frac{\sum_{320}^{295} E_\lambda W_\lambda \Delta_\lambda}{\sum_{320}^{295} E_\lambda W_\lambda \Delta_\lambda} \qquad (3)$$

The above formulas may prove useful to the reader who is interested in providing safety criteria for the worker in a particular environment.

TABLE VIII RELATIVE EFFECTIVENESS OF THE LENS

ACTION SPECTRUM TO PRODUCE CATARACTS

Wavelength nm	Threshold Radiant Exposure - Lens Jcm^{-2}	Relative Efficiency
290	3.00	0
295	0.75	0.2
300	0.15	1.0
305	0.30	0.5
310	0.75	0.2
315	4.5	0.033
320	12.6	0.012
325	50.0	0

SUMMARY AND CONCLUSIONS

A 5000 w Xe-Hg source was used to produce 6.6 nm full-bandpass UV radiation through a double monochromator and 10.0 nm full-bandpass UV radiation through a single monochromator. Pigmented rabbit eyes and primate eyes were exposed to the ultraviolet radiant energy in 5-nm intervals from 290 nm to 323 nm and in 10-nm intervals from 325 nm to 400 nm. Corneal and lenticular damage was assessed and classified with a biomicroscope independently by two investigators.

The following conclusions can be drawn:

1. The action spectrum for corneal damage extends to about 320 nm. The action spectrum for UV-induced cataracts begins at 295 nm and extends to 320 nm. It was postulated that the absorption characteristics of the cornea were responsible for the cut-off wavelengths.

2. The most efficient waveband for the production of lenticular damage was 300 nm which gave a radiant exposure threshold H_L of 0.15 Jcm^{-2}.

3. All threshold lenticular radiant exposures produced lenticular opacities which were transient and disappeared in 24 hours to 2 weeks post-exposure.

4. Permanent lenticular damage occurred at radiant exposure levels approximately twice the threshold lenticular radiant exposure ($2 \times H_L$).

5. Corneal threshold radiant exposure H_C rises very rapidly from 0.005 Jcm^{-2} at 270 nm 54 to 30.0 Jcm^{-2} at 335 nm.

6. Radiant exposures of $2 \times H_C$ and above in the 295 nm to 325 nm wavelength range result in irreversible corneal damage. Corneal damage included stromal haze, stromal opacities, endothelial changes with a thickening of the cornea. Severe corneal damage was accompanied by secondary anterior uveitis which was characterized by ciliary injection, aqueous flare, and keratic precipitates formed on the endothelium. Anterior uveitis was not found with exposures at 315 nm to 325 nm and above until $4 \times H_C$ radiant exposures were achieved.

7. Preliminary studies on the primate (Galago senegalensis) at 300 nm gave a corneal threshold of 0.01 Jcm^{-2} and a lens threshold of about 0.12 Jcm^{-2}. The primate cornea appears to be slightly more sensitive to UV radiation than the rabbit cornea (0.05 Jcm^{-2}). The lens radiant exposures demonstrate little difference between the rabbit and this primate.

8. The data demonstrate that the cornea should provide protection against lenticular damage; however, high radiant exposures delivered in a short duration in the wavelength range from 295 nm to 320 nm could result in cataracts and transient corneal damage.

9. Areas of research which need to be pursued include:

   a. Ocular transmittance studies are needed in the 200 nm to 400 nm wavelength range.

   b. Subthreshold exposures given at different levels and at varying intervals of time will assist in establishing long term, low level exposure effects.

   c. Fluorescence studies of the ocular media are needed to establish the molecular changes resulting from UV exposure.

   d. UV exposures combined with the visible and infrared radiation exposures will establish synergistic or additive effects.

   e. The mechanisms of ultraviolet induced cataracts.

   f. The ocular effects of UV radiation in combination with photosensitizing drugs.

REFERENCES

1. Hogan, M. J., J. A. Alvarado and J. E. Waddell: Histology of the Human Eye: An Atlas and Textbook. W. B. Saunders, Philadelphia, 1971.

2. Boettner, E. A. and J. R. Wolter: Transmission of the ocular media. Invest. Ophth. 1(6):766-783, 1962.

3. Kinsey, V. E.: Spectral transmission of the eye to ultraviolet. Arch. Ophth. 39(4):508-513, 1948.

4. Kuwabara, T., J. H. Kinoshita and D. G. Cogan: Electron microscopic study of galactose-induced cataract. Invest. Ophthalmol. 8:133149, 1969.

5. Benedek, G. B.: Theory of transparency of the eye. Appl. Optics 10:459473, 1971.

6. Buchanan, A. R., H. C. Heim and D. W. Stilson: Biomedical effects of exposure to electromagnetic radiation. I. Ultraviolet. Wright-Patterson Air Force Base, Dayton, Ohio, May 1960. WADD Tech. Report 60-376.

7. Christner, C. A., et al: State-of-the-art study on visual impairment by high intensity flash of visible, infrared, or untraviolet light. Battell Memorial Institute, Columbus, Ohio, Jan. 1965. Report No. BAT-171-9.

8. Verhoeff, F. H., L. Bell and C. B. Walker: The pathological effects of radiant energy on the eye: an experimental investigation with a systematic review of the literature. Proc. Am. Acad. Sci. 51:630-818, 1916.

9. Trümpy, E.: Experimentelle Untersuchungen über die Wirking hochintensieven Ultravioletts and Violetts Zwischen 314 and 435.9 μμ Wellenlange auf das Auge unter Besonderer Berucksichtigung der Linse. Albrecht von Graefes. Arch. Ophthal. 115:495-514, 1925.

10. van der Hoeve, J.: Strahlen und Auge. Albrecht von Graefes. Arch. Ophth. 116:245-248, 1925.

11. Duke-Elder, Sir S.: The pathological action of light on the eye: 1. Action of the outer eye. Photophthalmia, Lancet, 1, 1137-1141, 1926.

12. Duke-Elder, Sir S.: Radiational injuries. Textbook of Ophthalmology, Vol. 6, C. V. Mosby, St. Louis, 1954, 6445-6579.

13. Buschke, W., J. S. Friedenwald and S. G. Moses: Effects of ultraviolet irradiation on corneal epithelium: mitosis, nuclear fragmentation, post-traumatic cell movements, loss of tissue cohesion. J. Cell Comp. Physiol. 26: 147-164, 1945.

14. Fischer, F. P., D. Vermeulen and J. G. Eymers: Uber die zue Schädigung des Auges nötige Minimalquantität von ultravioletten und infra roten. Licht-Arch. f Augenheilk, 109:462-467, 1935.

15. Bachem, A.: Ophthalmic ultraviolet action spectra. Am. J. Ophth. 41: 969-975, 1956.

16. Clark, R., S. Zigman and S. Lerman: Studies on the structural proteins of the human lens. Exp. Eye Res. 8:172182, 1969.

17. Lerman, S.: Lens proteins and fluorescence. Isr. J. Med. Sci. 8: 1583-1589, 1972.

18. Grover, D. and S. Zigman: Coloration of human lenses by near-UV photooxidized tryptophan. Exp. Eye Res. 13:7076, 1972.

19. Spector, A., D. Roy and J. Stauffer: Isolation and Characterization of an Age depicted polypeptide from human lens and nontryptophan fluorescence. Exp. Eye Res. 21:9-24, 1975.

20. Pirie, A.: Formation of N' Formylkynurenine in proteins from lens and other sources by exposure to sunlight. Biochem. J. 125:203-208, 1971.

21. Walrant, P., R. Santis and L.I. Grossweiner: Photosensitizing Properties of N' Formylkynurenine. Photochem Photobiol. 22:63-67, 1975.

22. Pirie, A.: The effects of sunlight on proteins of the lens, in Contemporary Ophthalmology. Edited by J. Bellows. Williams & Wilkins Pubishers, Balitmore, Maryland, 1971, pp. 484-493.

23. Zigman, S.: Eye lens color: formation and function. Science 171:807808, 1971.

24. Zigman, S., J. Schultz, T. Yulo and G. Griess: Possible Roles of near UV light in the cataractous process. Exp. Eye Res. 15:201-208, 1973.

25. Zigman, S., G. Griess, T. Yulo and J. Schultz: Ocular protein alterations by near UV light. Exp. Eye Res. 15:255-265, 1973.

26. Pirie, A.: The effects of sunlight on proteins of the lens, Contemporary Ophthalmology. Edited by J. Bellows. Williams & Wilkins, Baltimore, 1971.

27. van Heyningen, R.: Fluorescent compounds of the human lens, Ciba Symposium 19 (New Series). Elsevier, Amsterdam, New York, P. 151, 1973.

28. Kurzel, R. B., M. L. Wolbarsht and B. S. Yamanashi: Spectral studies on normal and cataractous intact human lenses. Exp. Eye Res. 17:6571, 1973.

29. Kurzel, R. B., M. L. Wolbarsht, B. S. Yamanashi, G. W. Staton and R. R. Borrman: Tryptophan excited states and cataracts in the human lens. Nature, 241:132133, 1973.

30. Zigman, S., J. B. Schultz, T. Yulo and D. Grover: Effects of near-UV irradiation on lens and aqueous humor proteins. Isr. J. Med. Sci. 8:1590-1595, 1972.

31. Zigman, S.: Eye lens color: formation and function. Science 171:807808, 1971.

32. Zigman, S., J. Schultz and T. Yulo: Cataract induction in mice exposed to near UV light. Ophth. Res. 6:259270, 1974.

33. Zigman, S. and T. Vaughan: Near UV light effects on the lenses and retinas of mice. Invest. Ophth. 13:462465, 1974.

34. Zigman, S. and S. J. Bagley: Near ultraviolet light effects on dogfish retinal rods. Exp. Eye Res. 12:155157, 1971.

35. Zigman, S., J. B. Schultz and T. Yulo: Possible roles of near UV light in the cataractous process. Exp. Eye Res. 15:201-208, 1973a.

36. Zigman, S., G. Griess, T. Yulo and J. Schultz: Ocular protein alterations by near UV light. Exp. Eye Res. 15:255-264, 1973b.

37. Pirie, A.: Colour and solubility of the proteins of human cataracts. Invest Ophthal. 7:634-650, 1968.

38. Harding, J. J. and K. J. Dilley: Structural proteins of the mammalian lens: A review with emphasis on changes in development, aging and cataract. Exp. Eye Res. 22:1-73, 1976.

39. Dilley, K. J. and A. Pirie: Changes to the proteins of the human lens nucleus in cataract. Exp. Eye Res. 19:59-72, 1974.

40. Buckingham, R. H. and A. Pirie: The effect of light on lens proteins in vitro. Exp. Eye Res. 14:297-299, 1972.

41. Griffin, A. C.: Methoxsalen in ultraviolet carcinogenesis in the mouse. J. Invest. Dermatol. 32:367-372, 1959.

42. Cloud, T. M., R. Hakim and A. C. Griffin: Photosensitization of the eye with methoxsalen. Arch Ophthalmol. 64:346351, 1960.

43. Cloud, T. M., R. Hakim and A. C. Griffin: Photosensitization of the eye with methoxsalen, II. Chronic effects. Arch. Ophthalmol. 66:689694, 1961.

44. Freeman, R. G. and D. Troll: Photosensitization of the eye by 8-methoxypsoralen. J. Invest. Dermatol. 53:449-453, 1969.

45. Egyed, M. N., L. Singer, A. Eilat and A. Shlosberg: Eye lesions in ducklings fed Ammi majus seeds. Zbl. Vet. Med. A. 22:764768, 1975.

46. Barishak, Y. R., A. M. Beemer, M. N. Egyed and A. Eilat: Histology of the retina and choroid in ducklings photosensitized by feeding Ammi majus seeds. Ophthal. Res. 8:169-178, 1976.

47. Parrish, J. A., T. B. Fitzpatrick, L. Tanenbaum and M. A. Pathak: Photochemotherapy of psoriasis with oral methoxsalen and longwave ultraviolet. New Eng. J. Med. 291:1207-1212, 1974.

48. MacKeen, D. S. Fine and B. S. Fine: Production of cataracts in rabbits with an ultraviolet laser. Ophth. Res. 5:317-324, 1973.

49. Ebbers, R. W. and D. Sears: Ocular effects of a 325 nm ultraviolet laser. Am. J. Optom. and Physiol. Optics 52:216-223, 1975.

50. Zuclich, J. A. and J. S. Connolly: Ocular damage induced by near ultraviolet laser radiation, Invest. Ophthal. 15, (9), 760-764, 1976.

51. Zuclich, J. A. and W. E. Kurtin: Oxygen dependence of near-ultraviolet induced corneal damage. Photochem Photobiol. 25:133-135, 1977.

52. Ham, W. T., H. A. Mueller and A. M. Clarke: Retinal sensitivity to damage from short wavelength light, in Symposium on Biologic Effects and Measurement of Light Sources. U. S. Dept. HEW Publication (FDA) 778002. BRH Rockville, Maryland, 1977, pp. 37-47.

53. Hiller, R., L. Giacometti and K. Yuen: Sunlight and cataract: An epidemiologic investigation submitted to Amer. J. Epidem., Oct. 1976.

54. Pitts, D. G. and K. R. Kay: The photo-ophthalmic threshold for the rabbit. Am. J. Optom. 46:561-572, 1969.

55. Pitts, D. G.: A comparative study of the effects of ultraviolet radiation on the eye. Am. J. Optom. 47:535-546, 1970.

56. Pitts, D. G. and T. J. Tredici: The effects of ultraviolet on the eye. Am. Ind. Hyg. Assoc. J. 32:235-246, 1971.

57. Pitts, D. G.: The human ultraviolet action spectrum. Am. J. Optom. and Physiol. Optics 51:946-960, 1974.

58. Pitts, D. G. and W. D. Gibbons: Corneal light scatter measurements of ultraviolet radiant exposures. Am. J. Optom. 50:187-194, 1973.

59. Pitts, D. G.: The ocular ultraviolet action spectrum and protection criteria. Health Physics 25:559-566, 1973.

60. NBS, State-of-Art uncertainties and limitations in UV radiometry, Optical Radiation News, No. 20, April 1977.

61. Cullen, A. P.: Ph.D. Dissertation, The City University, London, in preparation.

☆ U.S. GOVERNMENT PRINTING OFFICE: 1977— 757-057/6751

DEPARTMENT OF
HEALTH, EDUCATION, AND WELFARE
PUBLIC HEALTH SERVICE
CENTER FOR DISEASE CONTROL
NATIONAL INSTITUTE FOR OCCUPATIONAL SAFETY AND HEALTH
ROBERT A. TAFT LABORATORIES
4676 COLUMBIA PARKWAY, CINCINNATI, OHIO 45226

OFFICIAL BUSINESS
PENALTY FOR PRIVATE USE, $300

POSTAGE AND FEES PAID
U.S. DEPARTMENT OF H.E.W.
HEW 399

DHEW (NIOSH) Publication No. 77-175